Biotechnology and Bioprocess Engineering 21: 1-18 (2016)
DOI 10.1007/s12257-015-0733-5

REVIEW PAPER

Synthesis, Characterization, and Antibacterial Properties of Silver Nanoparticles-Graphene and Graphene Oxide Composites

Huifang Liu, Linlin Zhong, KyuSik Yun, and Monica Samal

Received: 24 November 2015 / Revised: 29 December 2015 / Accepted: 16 January 2016 / Published Online: 29 February 2016

Abstract In the field of nanotechnology, silver nanoparticles have been considered a promising antibacterial material for a century. The potential applications of graphene-based materials are increasingly recognized for their special physico-chemical and biological properties. In particular, graphene and graphene oxide as the foundation of nanocomposites have garnered much interest among researchers in many fields. In this review, we concentrate on different aspects of silver nanoparticle composites with graphene and graphene oxide, focusing on their synthesis methods, special characteristics, and antibacterial properties; we also briefly discuss limitations and future research.

Keyword: silver nanoparticles, graphene, graphene oxide, composites, synthesis, antimicrobial properties

1. Introduction

Metal nanoparticles (MNPs) have gained interest and are a focus in diverse areas of research, most importantly in biological fields such as antibacterial studies [1]. Many types of MNPs, such as copper [2], titanium [3], magnesium [4], gold [5], zinc oxide [6], and silver have been used in a variety of applications [7,8]. Silver nanoparticles (AgNPs), which have unique chemical and physical properties, are of particular interest because of their striking antimicrobial effectiveness against bacteria, viruses, and other microorganisms [7]. AgNPs have high surface and catalytic activities, and are widely used as catalysts [9]. Silver was first recognized for its antiseptic activity, which led to continued research into its antibacterial effects [10,11]. AgNPs are not only effective antimicrobial agents against gram-positive and gram-negative bacteria [12], but also have low toxicity to mammalian cells [11,13] at low concentrations, and thus are useful in biomedical applications. AgNPs play an important role in the development of a new generation of antibiotics, which will help to overcome drug resistance [11,14]. Metal nanoparticles are promising candidates for addressing the problem of multi-drug-resistant bacteria because microorganisms are much less likely to develop resistance to silver than to the antibiotics now widely used for medical, environmental, structural, electrical, and everyday purposes [11,15].

Several reports have proposed different possible mechanisms of silver's antibacterial efficacy. First, Ag^+ is released by Ag nanomaterials [16,17], which can bind to thiol groups with the help of bacterial enzymes and then affect bacterial DNA replication [18]. Similarly, owing to particle-specific interaction of AgNPs with bacteria, the penetration of Ag+ into a bacterial cell causes cell death [19,20]. Other possible antibacterial mechanisms may include the oxidative stress generated at the surface of AgNPs by reactive oxygen species (ROS) [21,22]. In sum, the antibacterial mechanism of silver is not completely understood, but it has mainly been attributed to the release of Ag^+ ions [20].

Upon coming into contact with oxygen, AgNPs are easily oxidized and release Ag^+ ions, which severely impairs the stability of AgNPs and makes them a potential environmental hazard [11,23]. AgNPs have diverse applications in the form of wound dressings, coatings for medical devices, and AgNP-impregnated textiles for the treatment of wounds

Huifang Liu, Linlin Zhong, KyuSik Yun*, Monica Samal*
Department of BioNano Technology, GBRI, Gachon University, Seongnam 13120, Korea
Tel: +82-31-750-8983
E-mail: samalmonica@gachon.ac.kr/ms.phd.sci@gmail.com
Tel: +82-31-750-8753
E-mail: ykyusik@gachon.ac.kr

and burns [24]. However, choosing a starting material is a challenge because of the high price of silver and its chemical properties [25,26]. These are the main limitations to the synthesis of AgNPs and their subsequent applications. However, such limitations do not prevent researchers from intelligently utilizing the antibacterial activities of AgNPs endowed with desirable parameters like size, shape, and reactivity of AgNPs with relatively large surface areas.

With the development of nanotechnology, another exciting family of materials, graphite, has been discovered and used by researchers all over the world [27]. Graphite is a crystalline form of carbon, a semimetal, a native element mineral, and one of the allotropes of carbon [28]. Graphite is the most stable form of carbon under ambient conditions [29]. Another important family member is graphene, obtained through the mechanical exfoliation of graphite or by a variety of other methods. While synthesizing graphene from graphite, an intermediate product, graphene oxide (GO), was discovered [111].

Graphene-related materials have unique thermal, electronic, and mechanical properties, and hold great promise for several potential applications, including as super-capacitors, nano-electronics, conductive thin films, nano-sensors, and nano-medicines [30]. Graphene has a large theoretical specific surface area of 2,630 m^2/g [30,31], high intrinsic mobility of 200,000 $cm^2/v/sec$, thermal conductivity of ~5,000/Wm/K [32], and optical transmittance of ~97.7%. Its good electrical conductivity is useful in the development of transparent conductive electrodes [28]. Since its discovery, graphene has been applied in many different fields of research [31]. In the biomedical field, functionalized graphenes have been used for different purposes, such as gene transfection [33,34], drug delivery [35], bio-sensing [36], photo-thermal therapy, and tumor imaging [37]. Recently, the potential antibacterial applications of graphene and graphene-based nano-composites have also attracted considerable interest, although whether and how GO acts as an antibacterial agent is still under debate [38]. However, the antibacterial activities of individual graphene nano-sheets or GO are limited [39]. At the same time, composite nanomaterials have begun to be utilized as therapeutic agents in many diseases [40]; these include polymer-coated nanoparticles [41], diamond–carbon nano-composites [42], composites of two or more nanomaterials [43], and heterostructures of MNPs on graphene/GO/reduced GO sheets [44,45]. Because of the high specific surface area and the surface functional groups of graphene-based materials, they are convenient foundations for MNPs [46]. The aggregation of MNPs usually inhibits their antibacterial effects, but the aggregation can be overcome by incorporation into graphene/GO-MNP hybrids [21]. In recent studies, graphene-metal-NPs-based nanocomposites have been fabricated, and most results show incredibly enhanced antibacterial properties [47]. The large surface area of GO and the direct growth of AgNPs on GO profoundly strengthens the antibacterial performance of the combined system through a synergistic effect [48] upon bacterial contact [49]. Fig. 1 illustrates the different methods of AgNPs-graphene composite synthesis. In this review, we concentrate on AgNP composites with graphene and GO, focusing on the different synthesis methods, characteristics, and antibacterial properties of the composites.

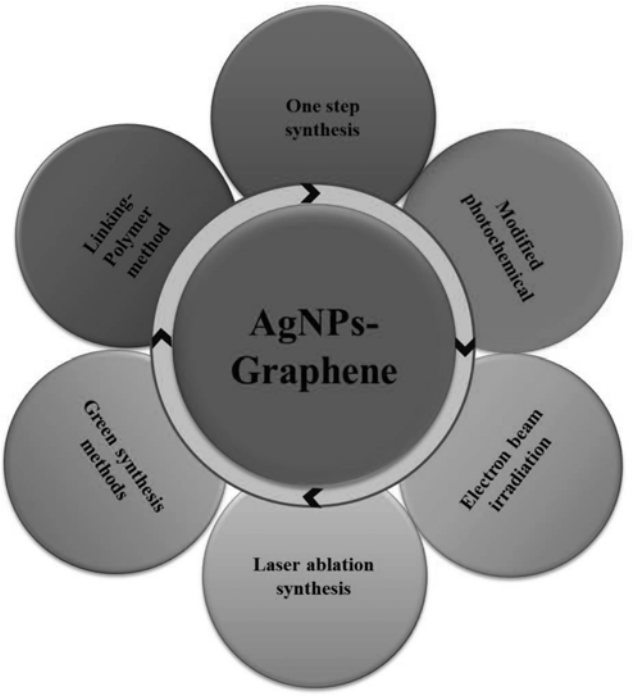

Fig. 1. Illustration of applications of Ag NPs - Graphene composites.

2. Synthesis of AgNPs

Many procedures for synthesizing metallic nanoparticles have been reported, such as salt reduction [50], microwave dielectric heating reduction [51], ultrasonic irradiation [52], radiolysis, solvothermal synthesis [53], electrochemical synthesis [54], *etc.* [49]. AgNPs synthesis [7] by physical [55] and chemical methods [56] is expensive and/or uses toxic chemicals [57] leading to pollution [58] and requiring modification of the synthesis processes. Hence, feasible, green methods to synthesize AgNPs [59] are attractive; these make use of microbes and plants [60]. We will focus on several common methods of synthesizing silver nanoparticles: chemical reduction [56], photo-reduction [61], laser ablation [62], irradiation, electrochemical [63], electrolysis plating [64], and biological/green synthesis [65].

2.1. Chemical reduction method

The chemical reduction method [56] involves reduction of the ionic salt in an appropriate medium in the presence of a surfactant using various reducing agents. The reaction time [5], reaction temperature [66], reaction pH [17], laser exposure [62], and electron beam strength [67] can be controlled to produce different structures, such as spheres [1], triangles [68], cubes [69], pentagons, and hexagons [70].

Li *et al.* [69] added 25 mL of 1×10^{-3} M silver nitrate ($AgNO_3$) aqueous solution containing 0.1 mL of 1×10^{-3} M n-dodecylthiol to equal volumes of 4×10^{-3} M $NaBH_4$ and 2.5×10^{-4} M sodium oleate solutions with vigorous stirring at 0°C. The resulting yellow-brown colloidal solution was stabilized by sodium oleate. It was then continuously stirred and warmed to room temperature. The solution was then heated to 80°C and cooled back to room temperature. In the process, excess $NaBH_4$ was decomposed. The schematic diagram for the self-assembly of AgNPs is shown in Fig. 2A, and the cubic AgNPs are shown in Fig. 2B.

$AgNO_3$ is the most popular metal salt precursor for the synthesis of AgNPs, though sliver chloride (AgCl) is also a choice. Reports on improvements in controlling the size and structure of AgNPs suggest using stabilizing agents [50], such as sodium dodecyl sulphate ($C_{12}H_{25}SO_4Na$) (SDS) [71] or sodium citrate [72]. Guzmán *et al*. used 8% (w/w) SDS as a stabilizing agent and hydrazine hydrate solution and sodium citrate solution ($C_6H_5O_7Na_3$) as reducing agents. $C_6H_5O_7Na_3$ was also used as a stabilizing agent at room temperature. The solution changed from a transparent colorless state to pale yellow and then to pale red when $C_6H_5O_7Na_3$ was used as stabilizing agent. This change in color indicated the formation of AgNPs [50]. Different types of organic polymers [73] have been used as dispersion agents to avoid aggregation of the Ag nanoparticles; such polymers include Poly-vinyl-Pyrrolidone (PVP) [74] and polyvinyl acetate (PVA) [75].

2.2. Photo-reduction method

In colloidal chemistry, the shape and morphology of nanoparticles are equally important as their size. A number of synthesis methods have been developed that enable control of these factors, of which photo reduction is well-described and effective. In 2007, Courrol *et al.* proposed a method using UV, LED, Xenon, and sodium lamps for excitation [61] to reduce the Ag salt. Separate solutions of 0.034 g $AgNO_3$ and 0.011 g acrylic in ethanol were stirred vigorously for 30 min. A 70W, high-pressure sodium lamp, a 150 W xenon lamp, and an ultraviolet LED were used to induce the reduction of Ag^+ and form a colloidal suspension of AgNPs. Second harmonic Nd:YAG coherent laser pulses, at a wavelength of 532 nm with 15 ~ 200 mJ pulse energy, 10 ns duration, and a repetition rate of 10 Hz, were also employed to synthesize NPs. This method provides a novel and easy way to prepare AgNPs of defined size and shape using polymerizable resin, visible illumination, and laser irradiation [61]. The absorption spectra and TEM images of AgNPs obtained using different irradiation sources are shown in Fig. 3. It is important to mention that reducing agents can also act as stabilizing agents. Xu *et al.* synthesized AgNPs with time-dependent UV irradiation of $[Ag(NH_3)_2]^+$ aqueous solution using poly(N-vinyl-2-pyrrolidone) as both a reducing and a stabilizing agent [78]. Figs. 4A and 4B show the TEM images of silver NPs formed with different durations of UV irradiation. Fig. 4C demonstrates the X-ray diffraction spectra of AgNPs and Fig. 4D shows the absorption spectra of AgNPs formed from silver oxide given different durations of UV irradiation.

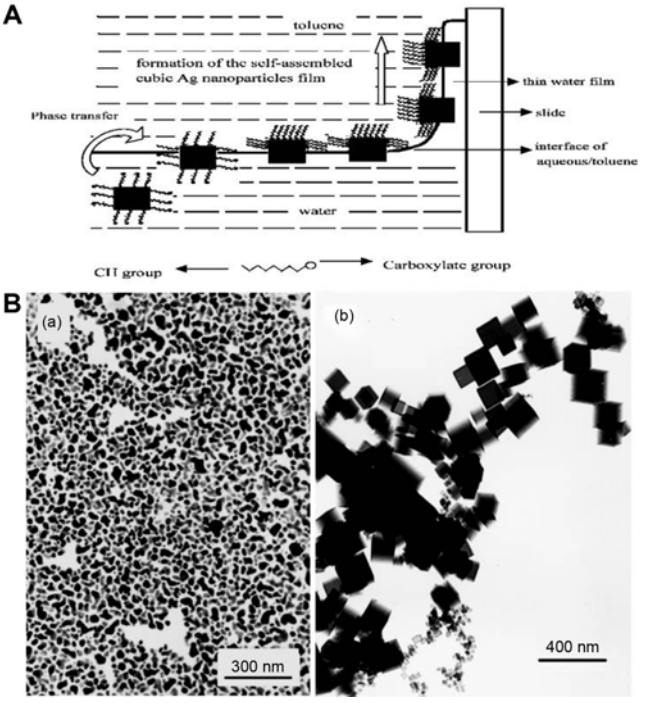

Fig. 2. (A) The schematic diagram of the film fabrication of self-assembled cubic Ag NPs. (B) The TEM images of (a) non-thiol and (b) thiol-bonded Ag NPs. Reprinted with permission from reference [69], copyright Thin Solid Films 460 (2004) 78-82.

UV irradiation-based AgNP preparation is easy and environmentally friendly. It is a simple method that allows for easy metal complex precursor synthesis and produces aqueous dispersions of metal nanoparticles [79].

2.3. Laser ablation method

Laser ablation has been used to prepare stable AgNPs. The importance of such a method is that the surfactants fully cover the nanoparticles and hence avoid direct nanoparticle contact and subsequent aggregation [62]. Fumitaka *et al.*

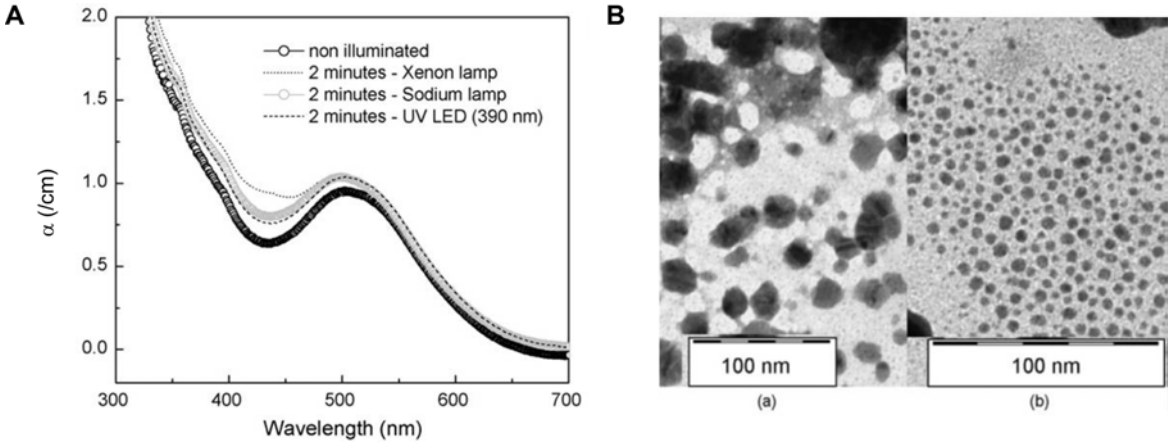

Fig. 3. (A) Absorption spectra of a colloidal solution upon 2-min illumination with non-focused xenon light (XeNPs), sodium light (NaNPs) and UV LED (390 nm) (LEDNPs) and a non-illuminated solution. (B) TEM images of silver particles obtained from: (a) $AgNO_3$ solution and auto-polymerizable resin in ethanol kept in the dark for 12 h followed by exposure to xenon lamp for 15 min; (b) after photolysis of the same solution by 5 min of laser excitation with 532 nm (200 mJ, 10 Hz) laser. Reprinted with permission from reference [61], Colloids and Surfaces A: Physicochemical and Engineering Aspects 305 (2007) 54-57.

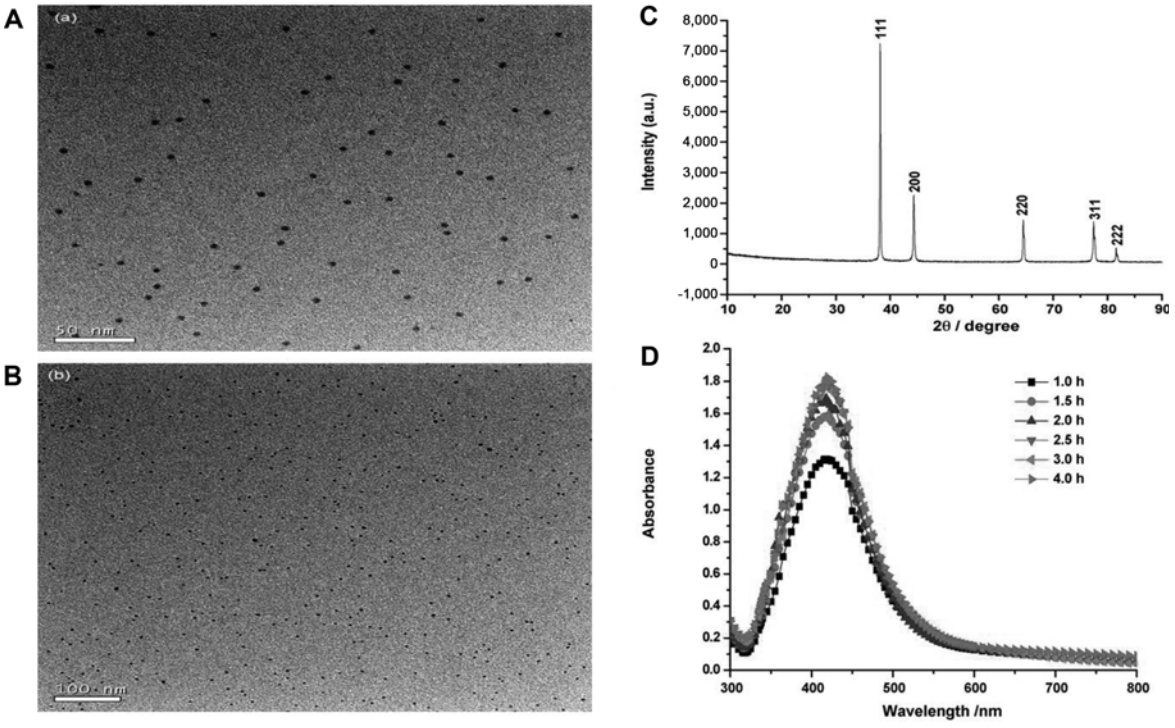

Fig. 4. (A, B) TEM images of silver NPs at different times of UV irradiation. (C) X-ray diffraction spectra of Ag NPs. (D) Absorption spectra of Ag NPs from silver oxide at different times of UV irradiation. Reproduced with permission from reference [78], copyright Colloids and Surfaces A: Physicochem. Eng. Aspects 320 (2008) 222-226.

prepared AgNPs by laser ablation of a metal silver plate in an aqueous solution of SDS. Briefly, the metal plate was placed on the bottom of a glass vessel filled with 10 mL of SDS solution. The metal plate was irradiated by the focused output of the second harmonic (532 nm) of a Quanta-Ray GCR-170Nd:YAG laser using a lens with a focal length of 250 mm. The spot size of the laser beam on the surface of the metal plate was varied in diameter by changing the distance between the lens and the metal plate. Upon irradiation, the solution steadily became a brownish-yellow color. Fig. 5A shows the schematic diagram of the experimental setup used to synthesis AgNPs *via* laser ablation. The absorption spectrum (Fig. 5B) shows a peak at 400 nm with a broad band in the UV domain, which is

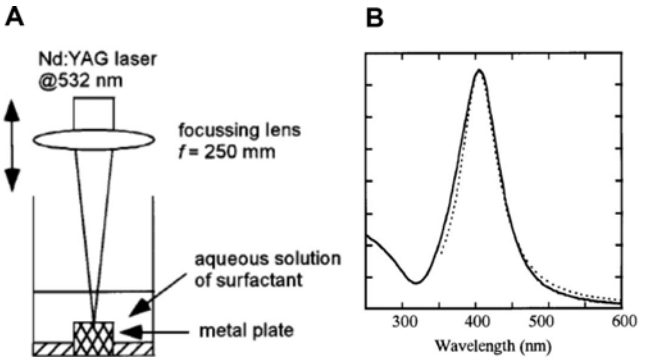

Fig. 5. (A) Schematic diagram of the experimental setup and (B) absorption spectrum (UV-Vis) of Ag NPs in 0.01 M SDS solution. Reproduced with permission from reference [62], copyright J. Phys. Chem. B 2000, 104, 9111-9117.

similar to the absorption spectra of AgNPs obtained by the chemical reduction of Ag salts in reversed micelles [80,81]. Threshold laser power, density of NPs, and size of NPs are proportional to laser power and inversely proportional to SDS concentration [62].

In other works, it has been reported that AgNPs can survive longer in anionic SDS than in cationic cetyl trimethyl ammonium bromide (CTAB) as the static properties of the surfactants have a significant impact on the formation of AgNPs. This is also related to the possibility of double layers of surfactant forming on the nanoparticles. Doubly negatively charged $-SO_4^{2-}$ groups remain oriented towards positively charged Ag, leading to interpenetration of surfactant and stabilization of AgNPs, whereas such a phenomena is not possible with $-N(CH_3)_3^+$ in CTAB [82]. Using the laser ablation technique with high laser power, small laser beam spot size, and the aid of surfactants, small AgNPs in pure water without any chemical additives were obtained [83].

K *et al*. [84] reported an efficient method for the synthesis of AgNPs in aqueous solutions of PVA at different concentrations by the laser ablation method and compared the sizes and properties of the NPs in PVA solutions versus those in water alone. PVA has advantages over water in the respect that no reducing agent is necessary in PVA and the AgNPs are protected by PVA fractions. The average sizes of well-dispersed spherical AgNPs in 1, 3 and 4% PVA solutions are 6.13, 6.86 and 3.99 nm, respectively, with 4% PVA solution yielding the minimum size. The UV-vis absorption of the AgNPs from various solutions show that the peak arising from the LSPR (localized surface plasmon resonance) appears at 400 nm with a broad peak in the UV region that can be assigned to inter-band electron transitions. It is interesting to note that the maximum intensity of the LSPR peak occurs in 4% PVA solution.

2.4. Irradiation method

Microwave irradiation [11], electron irradiation, γ –irradiation [84], sunlight irradiation, and UV irradiation have been used to synthesize AgNPs and control their size and structure [85]. Henglein and Giersig [86] investigated the γ-radiolytic reduction of $AgClO_4$ in a solvent comprised of alcohol and water in the presence of citrate at different concentrations ($5.0 \times 10^{-5} \sim 1.5 \times 10^{-3}$ M) and the capping effect of citrate on Ag^+ ions. The mechanism of the formation of AgNPs obtained by gamma-irradiation of $AgNO_3$ in aqueous solution containing 6 M propanol and PVP at concentrations ranging from 0.2 to 5% has been reported [87]. The AgNPs so produced have a very narrow size distribution, 8.5 ± 1.7 nm (Fig. 6).

Bogle *et al*. [88] electron-irradiated a mixture of $AgNO_3$ and PVA with 6 MeV electrons to obtain AgNPs 10 ~ 60 nm in size for the first time. These NPs have face-centered

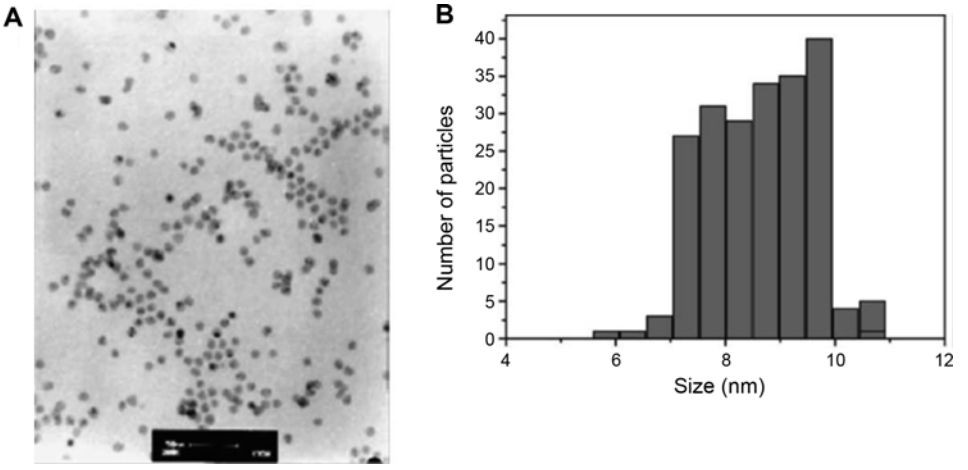

Fig. 6. TEM image (A) and size distribution (B) of PVP stabilized silver NPs. Reproduced with permission from reference [87]. Copyright Journal of Colloid and Interface Science 274 (2004) 89-94.

cubic structures and are spherical in shape, as seen on SEM images. A rapid, simple, and environmentally friendly method of biosynthesizing AgNPs *via* microwave irradiation of an $AgNO_3$ solution and *Bacillus subtilis* supernatant solution was reported by Saifuddin *et al*. [11]. These NPs are of average size (5 ~ 60 nm) and remain stable for several months. According to the authors, this is a better protocol for the synthesis of AgNPs than the electrochemical method. Sunlight-irradiation-mediated synthesis of AgNPs from a mixture of $AgNO_3$ and citrus lemon extract at room temperature was reported by Prathna *et al*. [89]. The reaction only took 4 h to produce spherical and spheroidal shaped NPs of sizes below 50 nm. The authors proposed a mechanism according to the following equation:

$$4Ag^{+} + C_6H_5O_7 + X + 2H_2O \rightarrow 4\ Ag^{0} + C_6H_5O_7H_3 + H^{+} + Y + O_2$$

X and Y are the unknown compounds in lemon juice and in the reaction mixture, respectively. The authors have suggested that the organic compounds probably had a role in stabilizing the AgNPs.

2.5. Biological-green synthesis method

The environmentally friendly nature of biosynthetic methods [66,90] for the creation of AgNPs are gaining focus. Biological templates [91] have been used to synthesize anisotropic AgNPs by self-assembly. Over the past several years, plants [92], algae, fungi [60], bacteria, and viruses [55] have been used for the production of low-cost, energy-efficient, and nontoxic NPs [59]. For example, to prepare biomass for biosynthesis of NPs, fungus was grown aerobically in a liquid medium containing (g/L) KH_2PO_4, 7.0: K_2HPO_4, 2.0; $MgSO_4{\cdot}7H_2O$, 0.1; $(NH_4)_2SO_4$, 1.0; yeast extract, 0.6; and glucose, 10.0. The flasks were injected, incubated on an orbital shaker at 25°C, and shaken at 150 rpm. The biomass was harvested after 72 h of growth by passing it through a plastic sieve, followed by a thorough washing with distilled water to remove any medium [93]. AgNPs were synthesized quickly using this biomass. The UV–visible spectrum showed a peak at 420 nm corresponding to the plasmon absorbance of AgNPs [93].

3. Synthesis of Graphene and Graphene oxide

3.1. Graphene

Motivations for graphene synthesis include its popularity, low price, the possibility for large-scale production [96], easy stabilization and transport, and an environmental friendly synthesis process [97]. Various methods have been used to make graphene, including micro-mechanical cleavage [98], anodic bonding [99], photo-exfoliation [97], solid phase exfoliation [100], growth on SiC [101,102], precipitation from metal, chemical vapor deposition [103], molecular beam epitaxy [104], and chemical synthesis [105]. Blakely studied the thermodynamics of growth of 'monolayer graphite' and of 'bilayer graphite' on crystals [28]; his 'monolayer graphite' continues to play a major role to this day. A more recent study reported the growth of epitaxial graphene on SiC wafers at high temperatures, which was used to prepare wafer-size graphene sheets with carrier mobility values of about 2,000 $cm^2/V/sec$ [106]. The direct growth of graphene on metal oxide surfaces is an exciting challenge that could benefit the nanoelectronics field. Several reports also include micromechanical exfoliation [107] and lithographically patterned pillars with AFM cantilever [108]. Though micromechanical exfoliation can produce high-quality graphene with outstanding electrical properties, it cannot be used for large-scale production. Exfoliation of graphite in solvents leads to the production of graphene oxide dispersions [109] which are then further reduced to obtain reduced graphene oxide. Many other substrate-free gas-phase synthesis methods for graphene platelets and multi-layered graphene have been reported, which made use of a microwave reactor and an arc-discharge method, respectively [110].

3.2. Graphene oxide

Comprehensive reviews on the preparation of dispersions of graphene oxide platelets and reduced graphene oxide platelets, made from GO, have recently appeared [28]. Generally, GO synthesis can use the Brodie, Staudenmaier, or Hummers methods. These three methods involve the oxidation of graphite. Brodie and Staudenmaier used a certain combination of potassium chlorate ($KClO_3$) with nitric acid (HNO_3) to oxidize graphite, while Hummers [111] used potassium permanganate ($KMnO_4$) and sulfuric acid (H_2SO_4) for the same purpose. Graphite salts made by intercalating graphite with strong acids, such as H_2SO_4, HNO_3, or $HClO_4$, have also been used as precursors that are subsequently oxidized to GO [36-39].

GO is extensively used for antibacterial studies. The polar oxygen functional groups on the surface of GO make it hydrophilic and dispersible in water. When treated with several reducing agents, such as hydrazine, hydroquinone, sodium borohydride ($NaBH_4$), and ascorbic acid, these dispersed solutions form reduced graphene oxide. The thorough chemistry of oxidation and reduction and the chemical tuning of graphene oxide are rapidly evolving areas of research. So far, the antibacterial activity of GO has been confirmed only using scanning electron microscopy (SEM), atomic force microscopy (AFM), and transmission electron microscopy (TEM). This is a limitation of this important area of research; GO should be studied on the

molecular level as well in order to better elucidate its antibacterial properties [36,111].

4. Synthesis of Ag-Graphene/GO Composites

The antibacterial properties of Ag renders it useful in treating wounds and other ailments [112]. Ag is cytotoxic to numerous microorganisms. However, the biomedical applications of Ag are limited as the release of the silver ion is slow or very fast depending on the source [113]. AgNPs with high specific surface area have enhanced antibacterial properties when compared to bulk Ag or silver salts. Graphene-based materials also have been shown to have strong antibacterial properties [27,114-116]. A great enhancement in antibacterial capacity is reported when a hybrid structure of AgNPs and graphene derivatives are used [117]. There have been outstanding developments in synthesizing these composites using many different methods. We will focus on some of the important ones.

4.1. One-step synthesis of silver graphene composites

A simple method for the synthesis of water-dispersible FG/Ag (FG = functional graphene) begins with stirring of a well-dispersed FGO (functionalized graphene oxide) with N-(trimethoxysilylpropyl) ethylenediaminetriacetic acid trisodium salt (TETA) in water with $AgNO_3$ solution at room temperature. The reaction mixture is then heated in an autoclave for 6 h at 140°C followed by separation of the solid by centrifuge and drying in an oven at 80°C. This method requires no surface modifiers or reducing agents. Fig. 7 shows the reaction scheme [119]. The antibacterial activities of FG/Ag formed in this manner were assessed by testing its effects on *E. coli* bacteria in comparison with those of GO and FGO. The FG/Ag composite was found to completely inhibit bacterial growth (Fig. 8).

4.2. Modified photochemical method

GO/Ag composites have demonstrated quite good antibacterial properties in the short term, but their long-term stability and antibacterial properties have not been evaluated fully

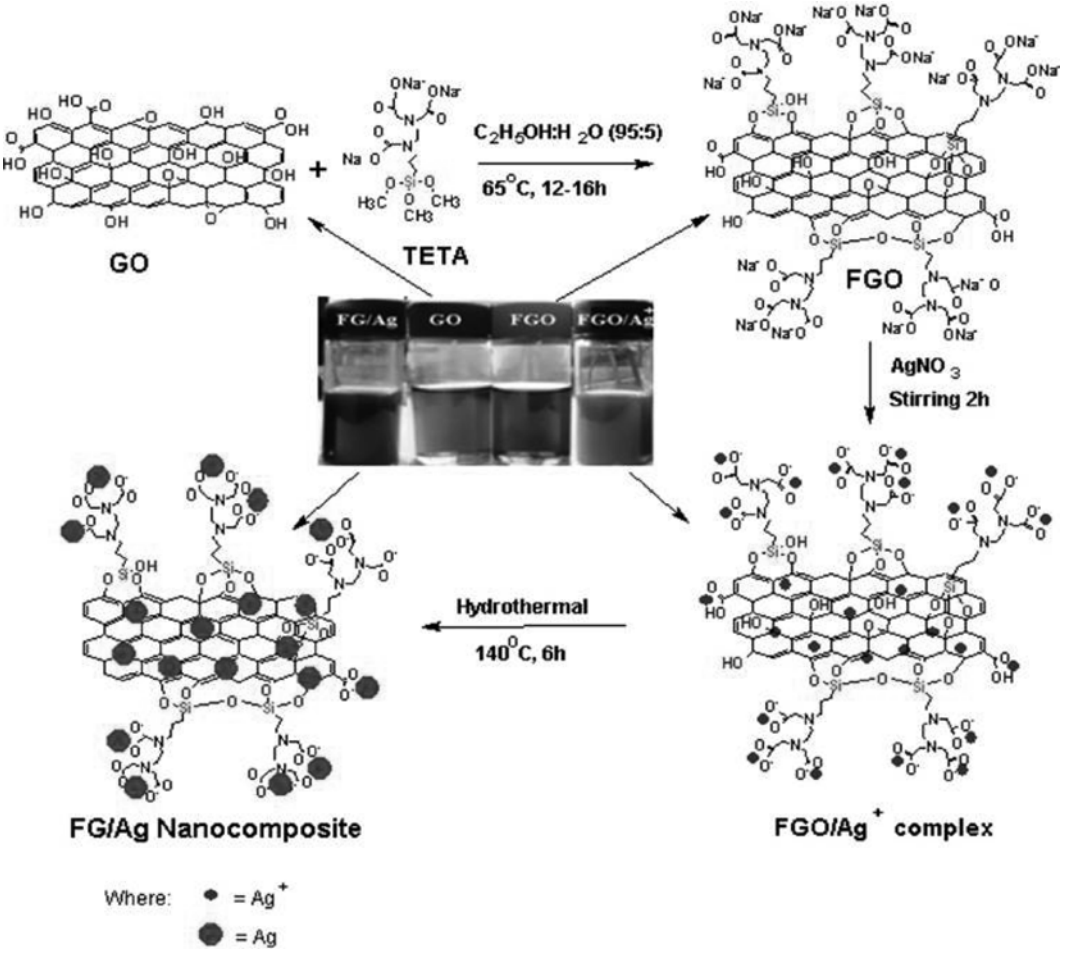

Fig. 7. Schematic diagram of the preparation of FG/Ag nanocomposite by a hydrothermal reduction route. Reproduced with permission from reference [119]. Copyright Sensors and Actuators B 181 (2013) 885-893.

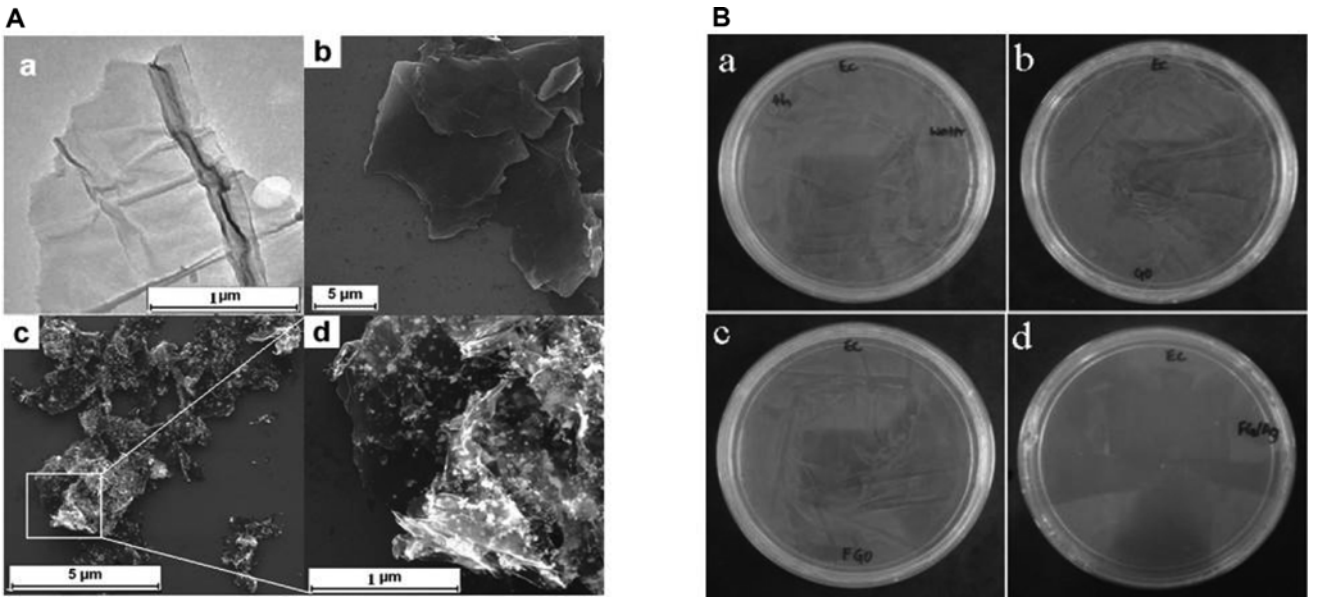

Fig. 8. (A) (a)TEM image of functionalized GO, FESEM images of (b) functionalized graphene after reduction, (c) and (d) Ag-NPs on FG at low and high magnifications, (B) digital photographs of E. coli colonies grown on agar plates with (a) water (control), (b) GO, (c) FGO, and (d) FG/Ag. Reproduced with permission from reference [118]. Copyright Sensors and Actuators B 181 (2013) 885-893.

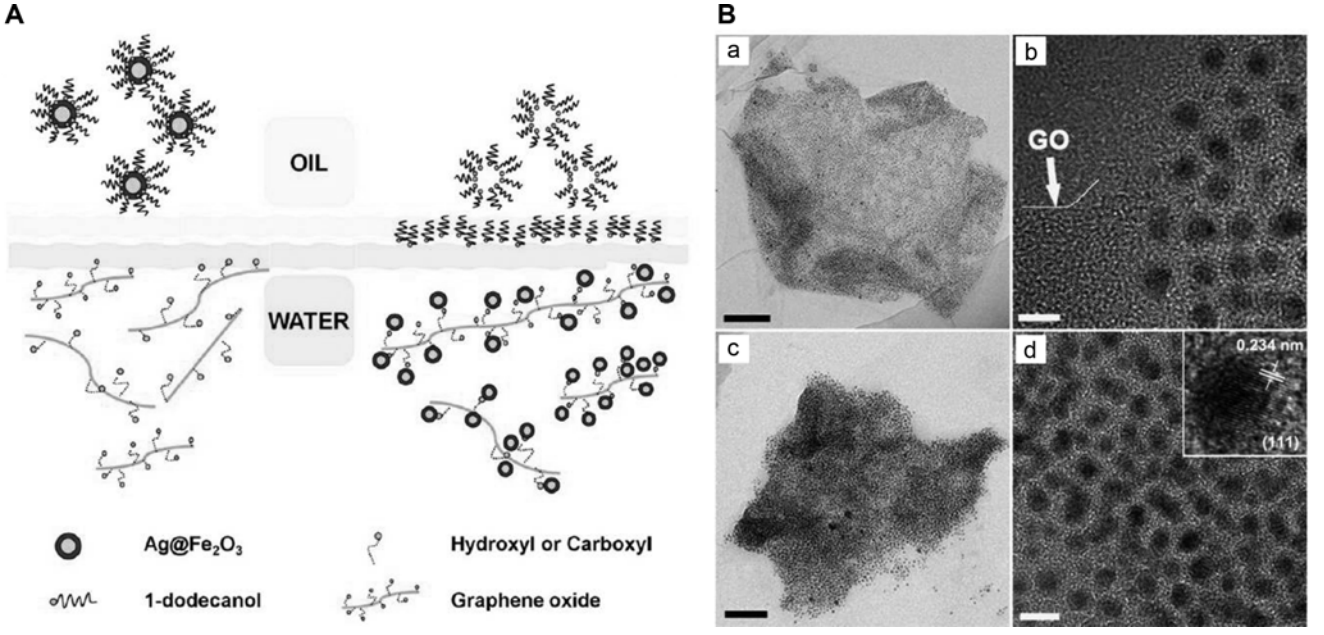

Fig. 9. (A) Schematic diagram of the phase transfer method of formation of Ag@Fe_2O_3-GO nanocomposites, (B) (a) TEM and (b) HRTEM images of Ag@ Fe_2O_3-GO NCs, (c) TEM and (d) HRTEM images of Ag@ Fe_2O_3-GO NCs after 7days. The black scale bars in (a) and (c) are 100 nm, and the white scale bars in (b) and (d) are 10 nm. The lattice spacing of the core Ag NPs corresponding to (111) plane is shown in the inset in (d). Reproduced with permission from reference [48]. Copyright ACS Appl. Mater. Interfaces 2013, 5, 11307-11314.

[36,120-127]. In an attempt to synthesize potential antibacterial GO composites with AgNPs, Jiang's group [48] fabricated Ag@Fe_2O_3-GO nanocomposites. Hydrophobic Ag@Fe_2O_3 NPs with 2 nm Ag cores were first synthesized according to a published method [128]. The oil dispersion of Ag@Fe_2O_3 NPs was stirred with an aqueous GO solution to produce a phase transfer reaction, followed by separation from unreacted Ag@Fe_2O_3 NPs as shown in Fig. 9A. Fig. 9B shows the Ag@Fe_2O_3 NPs-decorated GO sheet.

The antibacterial effects of Ag@Fe_2O_3-GO composites

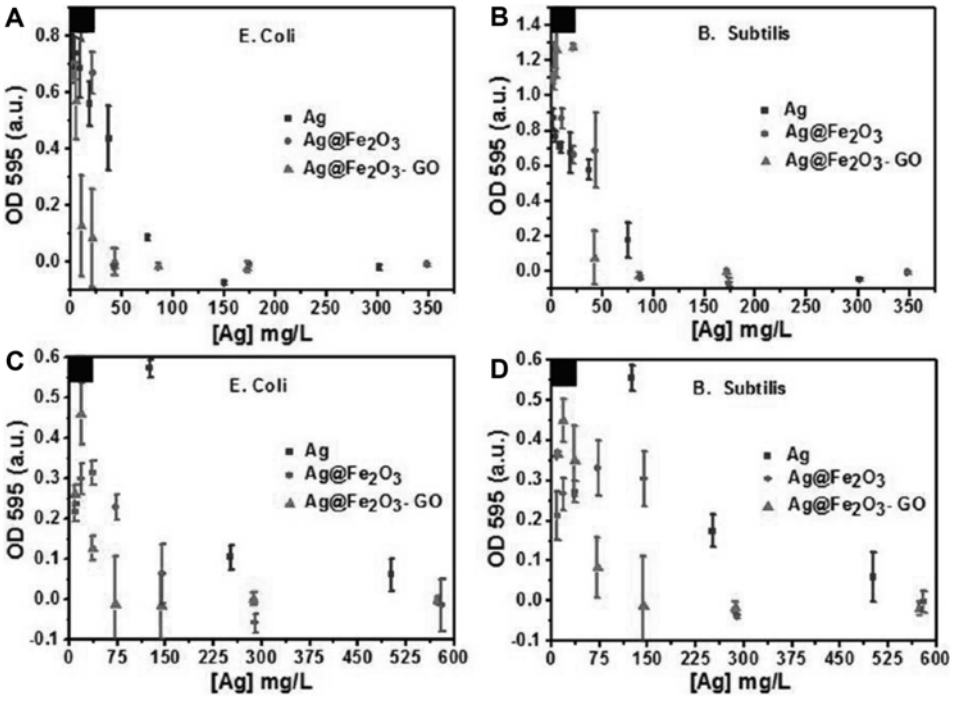

Fig. 10. Antibacterial activities against (A) E. coli and (B) B. subtilis after 18 h of incubation at 37°C with different concentrations of Ag NPs, Ag@ Fe_2O_3, and Ag@ Fe_2O_3-GO. (C, D) After 19 days of dialysis, Ag, Ag@ Fe_2O_3, and Ag@ Fe_2O_3-GO were used again for incubation with the bacteria strains under similar conditions. The standard deviations of the measurements are indicated by error bars (n = 3). Reproduced with permission from reference [48]. Copyright ACS Appl. Mater. Interfaces 2013, 5, 11307-11314.

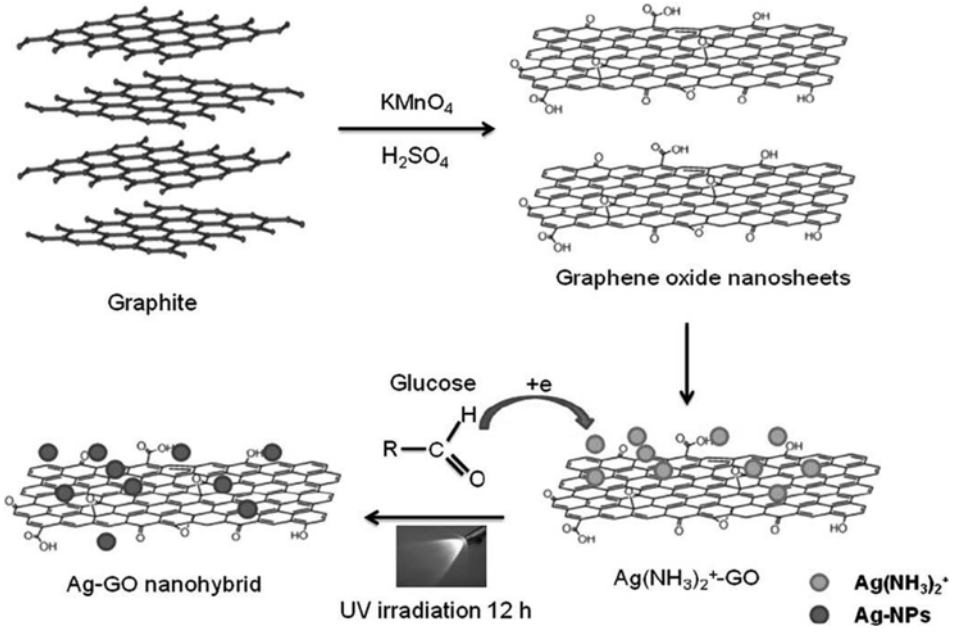

Fig. 11. Schematic diagram of a two-step route for the synthesis of the Ag-GO nanohybrid. Reproduced with permission from reference [129]. Copyright Journal of Alloys and Compounds 615 (2014) 843-848.

were investigated against gram-positive *B. subtilis* and gram-negative *E. coli.* Fig. 10 demonstrates the excellent antibacterial properties of Ag@Fe_2O_3 NPs and Ag@Fe_2O_3-GO composites and a comparison with Ag particles alone. The antibacterial properties were studied after 19 days, and it was observed that Ag@Fe_2O_3-GO nanocomposites are much more stable than either AgNPs alone or Ag@ Fe_2O_3 NPs, which can be attributed to the interface between the

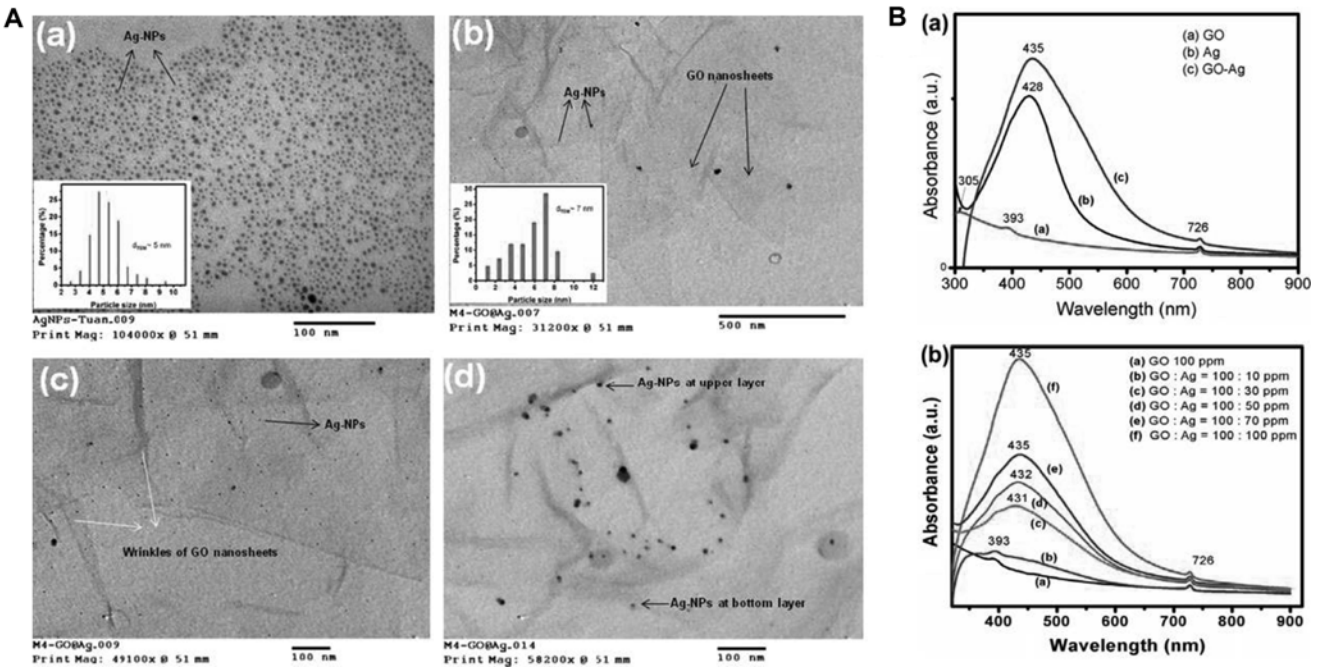

Fig. 12. (A) TEM images of (a) Ag NPs and (b-d) Ag-GO at different magnifications. (B) (a) The absorption spectra of GO, Ag NPs, and Ag-GO and (b) the absorption spectra of Ag-GO at different Ag concentration. Reproduced with permission from reference [129]. Copyright Journal of Alloys and Compounds 615 (2014) 843-848.

nanoparticles and GO sheets (Fig. 10).

Lan *et al*. [129] fabricated Ag-GO composites with a modified photochemical method. First, Ag_2O was prepared from $AgNO_3$ and NaOH, and then it was combined with NH_3 to give the amine complex. In the next step, oleic acid was added to the amine complex, and the reaction was mixed with a GO aqueous suspension and stirred for 30 min. The Ag species in the reaction mixture was then reduced by the addition of glucose and exposure to UV light. The AgNPs had deposited on GO sheets after 12 h of exposure. The synthesis scheme is shown in Fig. 11. The average size of the AgNPs on GO sheets were ~5 nm, and there was no aggregation. What had occurred was that the amine complex of Ag became attached to the GO sheets by electrostatic interactions, and then it was reduced to AgNPs by UV exposure. A TEM image (Fig. 12A) of the Ag-GO composite shows AgNPs on both the top and bottom layers of the sheets. The absorption intensity of the peak at 435 nm increases gradually with an increase in Ag concentration (Fig. 12B). The composite shows photoluminescence at 400 and 530 nm caused by the interaction between the LSPR of AgNPs and the natural photoluminescence of GO layers.

4.3. Electron beam irradiation method

In addition to their antibacterial applications, Ag-Graphene composites can also be used in electronic or electrochemical devices which require high conductivity. Jiao and Cheng's group [130] achieved such highly-conducting Ag-rGO composite films in a one-step synthesis process that uses electron beam radiation to simultaneously load AgNPs from $[Ag(NH_3)_2]^+$ and reduce graphene oxide. The synthesis scheme is shown in Fig. 13A. When the irradiation energy was increased to a certain point, the size of the AgNPs decreased, but beyond 500 KGy the size of the AgNPs increased. The size of the AgNPs formed by this method varies from 27.52 to 167.96 nm. The lowest resistivity of the composite film is 0.06 Ω (Fig. 13B). The authors suggested that this method is a simple, eco-friendly way to yield a high number of Ag-rGO composites and can be applied in biological fields.

4.4. Laser ablation synthesis method

In the laser ablation technique, AgNPs [83] are released to solution from an immersed ultra-pure Ag plate; this method requires no surface stabilizer or chemical reagent. Following this general principle, Sadrolhesseini *et al*. fabricated Ag-GO composites by immersing a pure Ag plate in GO aqueous solution and ablating it with a Q-switched Nd:YAG laser at room temperature for 10, 15, 30, and 60 min [131]. The particle size varied from 6 to 38 nm. The authors [131] also checked the thermal effusion of the composite, which is the exchange of heat with the environment. With an increase in the size of Ag NPs, thermal effusion increased.

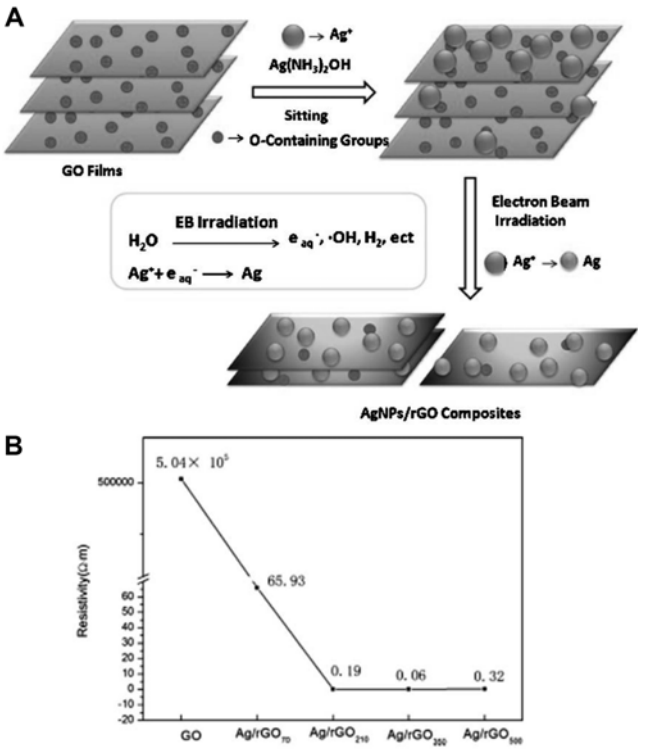

Fig. 13. (A) The synthesis scheme for the Ag NPs/rGO composites, (B) sheet resistance of GO and Ag NPs/rGO composites. Reproduced with permission from reference [130]. Copyright Applied Surface Science 349 (2015) 570-575.

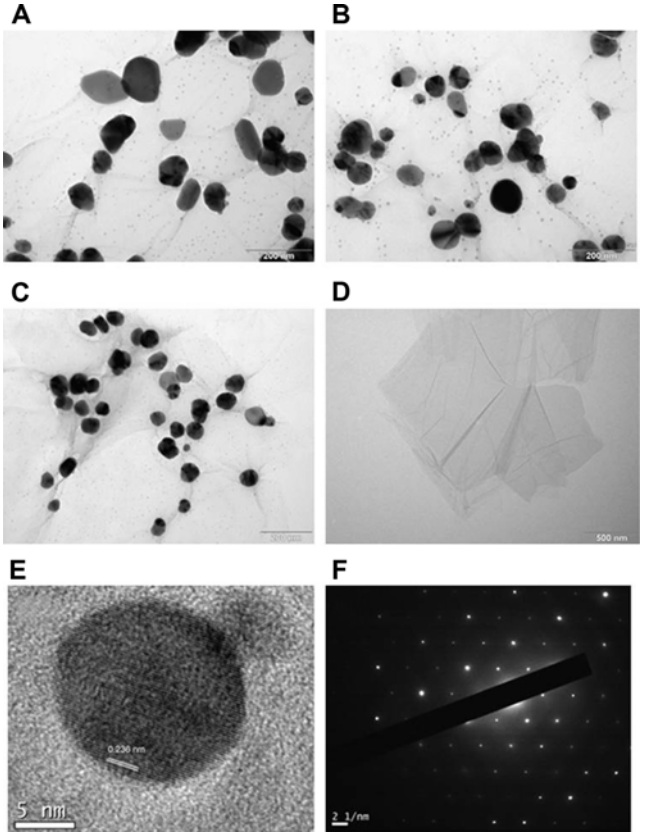

Fig. 14. TEM images of the Ag NPs on GO: (a) Ag NPs obtained from 0.6 M AgNO3, (b) Ag NPs obtained from 0.2 M AgNO3, (c) Ag NPs obtained from 0.1 M AgNO3, (d) TEM images of the GO sheets, (e) HRTEM image of Ag NPs obtained with 0.2 M AgNO3, and (f) SAED image of the Ag NPs obtained with 0.2 M AgNO3. Reproduced with permission from reference [132]. Copyright Acta Materialia 64 (2014) 326-332.

4.5. Green synthesis method

An environmentally friendly green synthesis method is desirable to avoid contamination with hazardous materials that causes health issues, the greenhouse effect, ozone depletion, acid rain, etc. Scientists around the globe are searching for new means of synthesizing MNPs. In fabricating the heterostructures of AgNPs-GO, non-hazardous substances like vitamin C, gelatin, and glucose are utilized as reducing and stabilizing agents. Li's group has used glucose as the reducing and stabilizing agent to fabricate AgNPs/GO composites. To a GO colloidal solution in water, glucose was added with stirring, followed by the addition of NH_3 and $AgNO_3$ solution. Finally, the product was isolated from the slurry by centrifugation and drying at 60°C in an oven. The electrochemical properties of tryptophan were studied using electrodes formed from AgNPs/GO composites. Hui *et al.* [132] synthesized AgNPs-GO composites by sonicating

Table 1. Summary of the synthesis conditions and the corresponding sizes of Ag nanoparticles on GO

Sample no.	Sample name	Experiment conditions				Ag particle size (nm)
		$AgNO_3$ (mol/L)	GO (mg)	Vitamin C (mmol/L)	Ultrasonic time (min)	
1	Ag-NPs-GO 0.6-30	0.6	20	5	30	20 ~ 120
2	Ag-NPs-GO 0.2-30	0.2	20	5	30	13 ~ 100
3	Ag-NPs-GO 0.1-30	0.1	20	5	30	45 ~ 55
4	Ag-NPs-GO 0.1-20	0.1	20	5	20	17 ~ 50
5	Ag-NPs-GO 0.1-10	0.1	20	5	10	35
6	Ag-NPs-GO 0.1-5	0.1	20	5	5	20 ~ 25
7	Ag-NPs-GO 0.1-1	0.1	20	5	1	15

Reproduced with permission from reference [132]. Copyright Acta Materialia 64 (2014) 326-332.

silver nitrate, GO solution, and vitamin C in an ultrasonication reaction at room temperature using different $AgNO_3$ concentrations and different sonication times [132].

Table 1 shows the size of the AgNPs under the different synthesis conditions. The particle size increases with increased $AgNO_3$ concentration and increased sonication time. However, with increased sonication time, the AgNPs are distributed more uniformly on the GO sheets, which can be attributed to Ostwald's ripening phenomenon. Fig. 14 shows TEM and HRTEM images of the AgNPs-GO composites.

Rapid thermal treatment to obtain pristine AgNPs/rGO composites has been reported by Zainy *et al.* [133]. The authors ground silver acetate and dry GO powder together into a fine powder, which they rapidly heated at 1,000°C for 20 sec in a preheated furnace in an ambient environment. No surfactant or stabilizer was used in the process. FESEM and TEM images show AgNPs 16.9 ± 3.5 nm in size uniformly distributed on the rGO surface (Fig. 15).

Zhang *et al.* reported the green synthesis of GO/Ag nanoprisms and their antibacterial efficacy [68]. Solutions of gelatin and $AgNO_3$ were stirred for 12 h to obtain Ag nanoprisms, then a dispersion of graphene oxide was added to the reaction mixture. The reaction mixture was then stirred for 12 h at room temperature, centrifuged, and dried at 60°C overnight. The reaction scheme is shown in Fig. 16A. TEM images of GO, GO-Ag nanoprisms, and silver nanoprisms are shown in Fig. 16B.

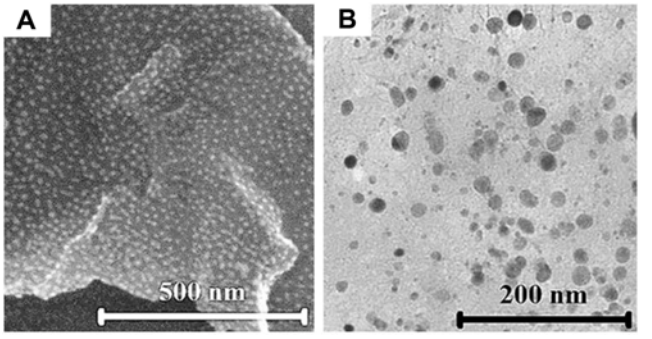

Fig. 15. (A) FESEM, (B) TEM images of rGO/Ag composite. Reproduced with permission from reference [133]. Copyright Materials Letters 89 (2012) 180-183.

The abilities of of GO and GO/Ag to inhibit the growth of *E. coli* were investigated; the results are shown in

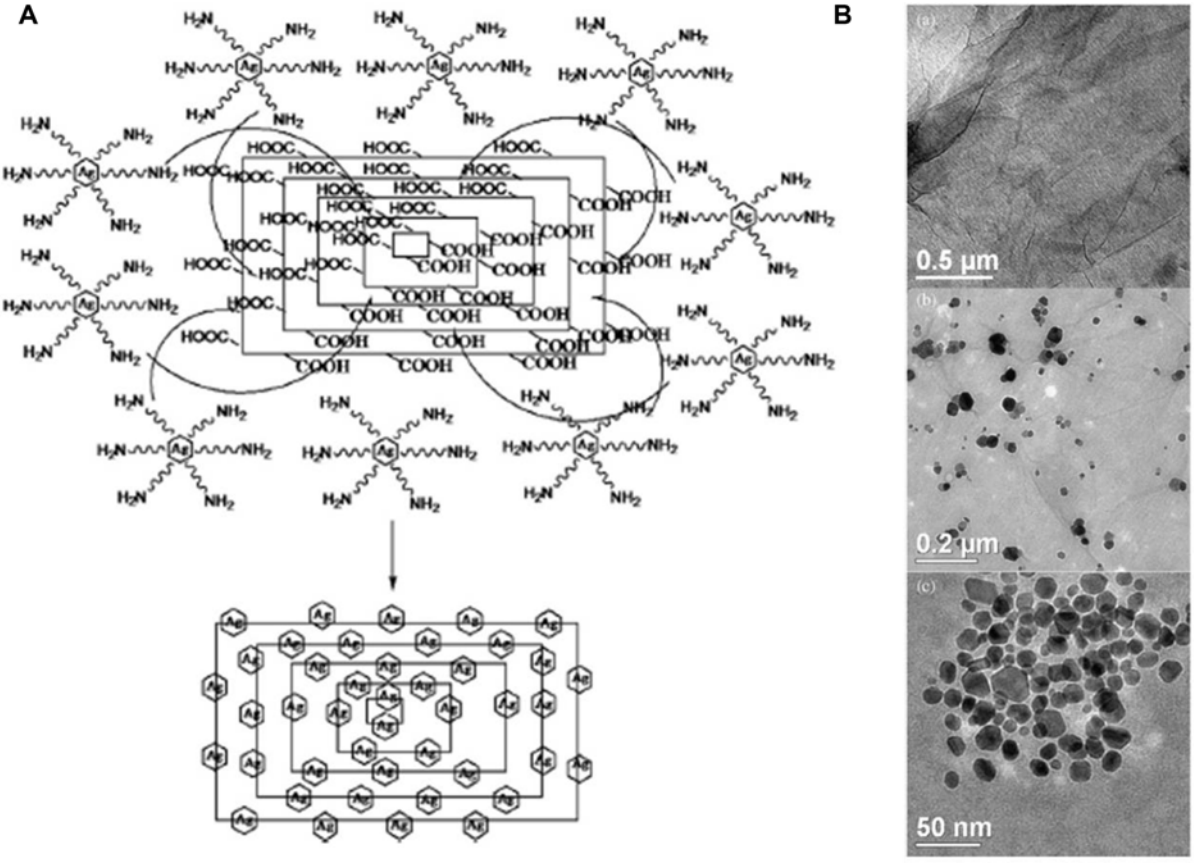

Fig. 16. (A) The schematics of the formation mechanism of silver nanoprisms decorated GO sheets. (B) The TEM of GO (a), GO-Ag nanoprism (b), and Ag nanoprisms (c). Reproduced with permission from reference [68]. Copyright Journal of Inorganic Biochemistry 105 (2011) 1181-1186.

Table 2. Growth inhibition rates of GO/Ag against *Escherechia Coli*

Growth inhibition rates (%)			
Concentrations	1 ppm	5 ppm	10 ppm
GO/Ag	73.1	85	99.9
GO	25.3	32	38

Reproduced with permission from reference [68]. Copyright Journal of Inorganic Biochemistry 105 (2011) 1181-1186.

Table 2. The results clearly indicate that GO/Ag has a very strong antibacterial effect. At a concentration of 10 ppm, GO/Ag inhibited the growth of *E. coli* by 99.9%; the effect decreased when the concentration of GO/Ag was decreased.

It is expected that this green approach to synthesizing AgNPs-GO/rGO/FG/FGO hybrids will lead to the development of a broad new class of MNPs-GO composites with excellent properties for many technological applications.

4.6. Linking polymer method

The linking polymer method involves the formation of metalloid polymer hybrid (MPH) nanoparticles bound to GO. Veerapandian *et al.* [134] reported an MPH, $Ag@SiO_2$, 12.5 ± 2 nm in size, which was coated with PEG and further silanized with 3-aminopropyl-triethoxysilane and then functionalized on GO (FGO) by covalent bonding. Fig. 17 shows the schematic illustration of fabrication of an FGO-based glucose biosensor and TEM images of GO, MPH, and FGO. The electrochemical properties and the amperometric glucose-sensing capability of FGO were also studied. The results suggest that FGO can be used for clinical biosensing applications.

Veerapandian and Neethirajan [135] synthesized GO decorated with Ag-Ru-chitosan hybrid nanoparticles (HNPs) and evaluated its immunosensing properties. First, Ag@[Ru(bpy)3]2+/chitosan HNPs were synthesized by a published method [136]. In the next step, the HNPs and an aqueous GO dispersion were stirred for 12 h, followed by isolation of the HNP-functionalized GO by centrifugation. The HNPs had an average size of 54 nm. To study the immunosensing properties of HNPs, first, an HNPs-Au electrode was fabricated. The HNPs-Au electrode was modified by treatment with glutaraldehyde in PBS (phosphate-buffered saline) in order to form an aldehyde layer on the

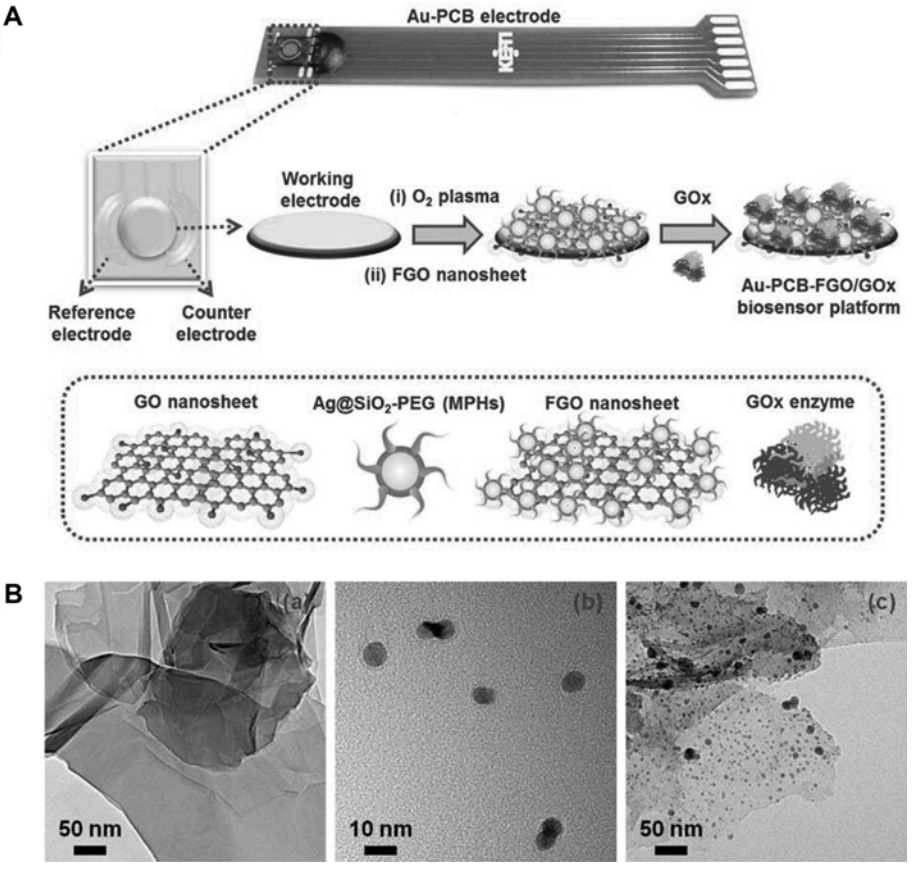

Fig. 17. (A) Schematic illustration of fabrication of FGO based glucose biosensor. (B) (a) HR-TEM image of nanosheets of GO, (b) MPHs, and (c) nanosheets of FGO. Reproduced with permission from reference [134]. Copyright Materials Research Bulletin 49 (2014) 593-600.

surface. The modified HNPs-Au electrode was immersed in anti-Lm (Lm = *L. monocytogenes*) solution to couple the aldehyde with anti-Lm. Excess antibody was removed by washing with PBS. The HNPs-Au/anti-Lm electrode was used to sense Lm bacteria in PBS and milk at various concentrations. Characterization shows a linear relationship between current change and Lm concentration. The presence of the bacteria Pa (*P. aeruginosa*) produced no response. Thus the HNPs-Au/anti-Lm immunosensor accurately detected the common food pathogen Lm.

Another heterostructure of AgNPs modified by poly (diallyldimethylammonium chloride, PDDA) and functionalized GO was reported by Wu *et al.* [137]. PDDA serves as an adhesive. The gram-negative bacteria *Escherichia coli* along with Gram-positive bacteria *Bacillus cereus* were chosen to investigate the antibacterial properties of the heterostructure. The antibacterial properties of the heterostructure were superior to those of AgNPs because of a synergistic effect between the different components of the heterostructure. Thus, the polymer linking method can produce three-dimensional heterostructural GO nanosheets decorated with multi-functional NPs with good electrochemical and biocompatible properties for biological applications.

5. Conclusion

This review represents a snapshot of the current state of AgNPs, GO, and AgNPs-Graphene/GO in antibacterial research. The synthesis methods we discussed give a clear indication of the importance of these amazing nanomaterials and their further development. For better bio-compatibility and lower toxicity, it will be necessary to clarify the mechanism behind antibacterial activity, which will require molecular-level studies. The high stability of the AgNPs-Graphene/GO nanostructures is responsible for their profound and long-term antibacterial activity. Novel synthesis methods for both graphene and silver nanoparticles will play a major role in future uses of these nano-composite materials.

Acknowledgement

This research was supported by the GRRC program of Gyeonggi province (2015-B03).

References

1. Hajipour, M. J., K. M. Fromm, A. A. Ashkarran, D. Jimenez de Aberasturi, I. R. de Larramendi, T. Rojo, V. Serpooshan, W. J. Parak, and M. Mahmoudi (2012) Antibacterial properties of nanoparticles. *Trends Biotechnol.* 30: 499-511.
2. Raffi, M., S. Mehrwan, T. M. Bhatti, J. I. Akhter, A. Hameed, W. Yawar, and M. M. ul Hasan (2010) Investigations into the antibacterial behavior of copper nanoparticles against *Escherichia coli*. *Ann. Microbiol.* 60: 75-80.
3. Elsaka, S. E., I. M. Hamouda, and M. V. Swain (2011) Titanium dioxide nanoparticles addition to a conventional glass-ionomer restorative: Influence on physical and antibacterial properties. *J. Dent.* 39: 589-598.
4. Al-Hazmi, F., F. Alnowaiser, A. Al-Ghamdi, A. A. Al-Ghamdi, M. Aly, R.M. Al-Tuwirqi, and F. El-Tantawy (2012) A new large–Scale synthesis of magnesium oxide nanowires: Structural and antibacterial properties. *Superlattices Microstruct*. 52: 200-209.
5. MubarakAli, D., N. Thajuddin, K. Jeganathan, and M. Gunasekaran (2011) Plant extract mediated synthesis of silver and gold nanoparticles and its antibacterial activity against clinically isolated pathogens. *Colloids Surf. B Biointerfaces* 85: 360-365.
6. Zhong, L. and K. Yun (2015) Graphene oxide-modified ZnO particles: Synthesis, characterization, and antibacterial properties. *Internat. J. Nanomed.* 10: 79.
7. Rai, M., A. Yadav, and A. Gade (2009) Silver nanoparticles as a new generation of antimicrobials. *Biotechnol. Adv.* 27: 76-83.
8. Marambio-Jones, C. and E. M. V. Hoek (2010) A review of the antibacterial effects of silver nanomaterials and potential implications for human health and the environment. *J Nanopart Res.* 12: 1531-1551.
9. Mitsudome, T., Y. Mikami, H. Mori, S. Arita, T. Mizugaki, K. Jitsukawa, and K. Kaneda (2009) Supported silver nanoparticle catalyst for selective hydration of nitriles to amides in water. *Chem. Commun. (Camb).* 3258-3260.
10. Mukherjee, P., A. Ahmad, D. Mandal, S. Senapati, S. R. Sainkar, M. I. Khan, R. Parishcha, P. V. Ajaykumar, M. Alam, R. Kumar, and M. Sastry (2001) Fungus-mediated synthesis of silver nanoparticles and their immobilization in the mycelial matrix: A novel biological approach to nanoparticle synthesis. *Nano Lett.* 1: 515-519.
11. Saifuddin, N., C. Wong, and A. Yasumira (2009) Rapid biosynthesis of silver nanoparticles using culture supernatant of bacteria with microwave irradiation. *J. Chem.* 6: 61-70.
12. Guzman, M., J. Dille, and S. Godet (2012) Synthesis and antibacterial activity of silver nanoparticles against gram-positive and gram-negative bacteria. *Nanomed.* 8: 37-45.
13. Mukherjee, S. G., N. O'Claonadh, A. Casey, and G. Chambers (2012) Comparative *in vitro* cytotoxicity study of silver nanoparticle on two mammalian cell lines. *Toxicol. In Vitro.* 26: 238-251.
14. Ramstedt, M., N. Cheng, O. Azzaroni, D. Mossialos, H. J. Mathieu, and W. T. Huck (2007) Synthesis and characterization of poly (3-sulfopropylmethacrylate) brushes for potential antibacterial applications. *Langmuir.* 23: 3314-3321.
15. Allison, B. C., B. M. Applegate, and J. P. Youngblood (2007) Hemocompatibility of hydrophilic antimicrobial copolymers of alkylated 4-vinylpyridine. *Biomacromol.* 8: 2995-2999.
16. Stewart, P. S. and J. William Costerton (2001) Antibiotic resistance of bacteria in biofilms. *The Lancet.* 358: 135-138.
17. Adolfsson-Erici, M., M. Pettersson, J. Parkkonen, and J. Sturve (2002) Triclosan, a commonly used bactericide found in human milk and in the aquatic environment in Sweden. *Chemosphere.* 46: 1485-1489.
18. Radheshkumar, C. and H. Münstedt (2005) Morphology and mechanical properties of antimicrobial polyamide/silver composites. *Mater Lett.* 59: 1949-1953.
19. Feuerstein, O., S. Matalon, H. Slutzky, and E. I. Weiss (2007)

Antibacterial properties of self-etching dental adhesive systems. *The J. Am. Dental Assoc.* 138: 349-354.
20. Choi, O., K. K. Deng, N. J. Kim, L. Ross, Jr., R. Y. Surampalli, and Z. Hu (2008) The inhibitory effects of silver nanoparticles, silver ions, and silver chloride colloids on microbial growth. *Water Res.* 42: 3066-3074.
21. Li, Y., W. Zhang, J. Niu, and Y. Chen (2012) Mechanism of photogenerated reactive oxygen species and correlation with the antibacterial properties of engineered metal-oxide nanoparticles. *ACS Nano.* 6: 5164-5173.
22. Li, Y., W. Zhang, J. Niu, and Y. Chen (2013) Surface-coating-dependent dissolution, aggregation, and reactive oxygen species (ROS) generation of silver nanoparticles under different irradiation conditions. *Environ. Sci. Technol.* 47: 10293-10301.
23. Quadros, M. E. and L. C. Marr (2010) Environmental and human health risks of aerosolized silver nanoparticles. *J. Air Waste Manage. Assoc.* 60: 770-781.
24. Silver, S., T. Phung le, and G. Silver (2006) Silver as biocides in burn and wound dressings and bacterial resistance to silver compounds. *J. Ind. Microbiol. Biotechnol.* 33: 627-634.
25. Wang, Y., Q. Yang, G. Shan, C. Wang, J. Du, S. Wang, Y. Li, X. Chen, X. Jing, and Y. Wei (2005) Preparation of silver nanoparticles dispersed in polyacrylonitrile nanofiber film spun by electrospinning. *Materials Lett.* 59: 3046-3049.
26. Panyala, N. R., E. M. Peña-Méndez, and J. Havel (2008) Silver or silver nanoparticles: A hazardous threat to the environment and human health. *J. Appl. Biomed.* 6: 117-129.
27. Liu, S., T. H. Zeng, M. Hofmann, E. Burcombe, J. Wei, R. Jiang, J. Kong, and Y. Chen (2011) Antibacterial activity of graphite, graphite oxide, graphene oxide, and reduced graphene oxide: Membrane and oxidative stress. *ACS Nano.* 5: 6971-6980.
28. Zhu, Y., S. Murali, W. Cai, X. Li, J. W. Suk, J. R. Potts, and R. S. Ruoff (2010) Graphene and graphene oxide: synthesis, properties, and applications. *Adv. Mater.* 22: 3906-3924.
29. Stankovich, S., D. A. Dikin, R. D. Piner, K.A. Kohlhaas, A. Kleinhammes, Y. Jia, Y. Wu, S. T. Nguyen, and R. S. Ruoff (2007) Synthesis of graphene-based nanosheets *via* chemical reduction of exfoliated graphite oxide. *Carbon* 45: 1558-1565.
30. dos Santos, C. A., M. M. Seckler, A.P. Ingle, I. Gupta, S. Galdiero, M. Galdiero, A. Gade, and M. Rai (2014) Silver nanoparticles: therapeutical uses, toxicity, and safety issues. *J. Pharm. Sci.* 103: 1931-1944.
31. Bitounis, D., H. Ali-Boucetta, B. H. Hong, D. H. Min, and K. Kostarelos (2013) Prospects and challenges of graphene in biomedical applications. *Adv. Mater.* 25: 2258-2268.
32. Shao, Y., J. Wang, M. Engelhard, C. Wang, and Y. Lin (2010) Facile and controllable electrochemical reduction of graphene oxide and its applications. *J. Mater. Chem.* 20: 743-748.
33. Feng, L., S. Zhang, and Z. Liu (2011) Graphene based gene transfection. *Nanoscale.* 3: 1252-1257.
34. Slowing, I. I., J. L. Vivero-Escoto, C. -W. Wu, and V. S. -Y. Lin (2008) Mesoporous silica nanoparticles as controlled release drug delivery and gene transfection carriers. *Adv. Drug Deliv. Rev.* 60: 1278-1288.
35. Sun, X., Z. Liu, K. Welsher, J. T. Robinson, A. Goodwin, S. Zaric, and H. Dai (2008) Nano-graphene oxide for cellular imaging and drug delivery. *Nano Res.* 1: 203-212.
36. Tang, J., Q. Chen, L. Xu, S. Zhang, L. Feng, L. Cheng, H. Xu, Z. Liu, and R. Peng (2013) Graphene oxide-silver nanocomposite as a highly effective antibacterial agent with species-specific mechanisms. *ACS Appl. Mater. Interfaces.* 5: 3867-3874.
37. Yang, K., S. Zhang, G. Zhang, X. Sun, S. T. Lee, and Z. Liu (2010) Graphene in mice: ultrahigh in vivo tumor uptake and efficient photothermal therapy. *Nano Lett.* 10: 3318-3323.
38. Pumera, M., A. Ambrosi, A. Bonanni, E. L. K. Chng, and H. L. Poh (2010) Graphene for electrochemical sensing and biosensing. *Trends Analyt. Chem.* 29: 954-965.
39. Nanda, S. S., G. C. Papaefthymiou, and D. K. Yi (2015) Functionalization of graphene oxide and its biomedical applications. *Crit. Rev. Solid State Mater.* 40: 291-315.
40. Yang, K., L. Feng, X. Shi, and Z. Liu (2013) Nano-graphene in biomedicine: theranostic applications. *Chem. Soc. Rev.* 42: 530-547.
41. Prabhu, S. and E. K. Poulose (2012) Silver nanoparticles: Mechanism of antimicrobial action, synthesis, medical applications, and toxicity effects. *International. Nano Lett.* 2: 1-10.
42. Purushotham, S. and R. V. Ramanujan (2010) Thermoresponsive magnetic composite nanomaterials for multimodal cancer therapy. *Acta Biomater.* 6: 502-510.
43. Ralchenko, V., A. Karabutov, I. Vlasov, V. Frolov, V. Konov, S. Gordeev, S. Zhukov, and A. Dementjev (1999) Diamond–carbon nanocomposites: Applications for diamond film deposition and field electron emission. *Diam. Relat. Mater.* 8: 1496-1501.
44. Zhou, X., X. Huang, X. Qi, S. Wu, C. Xue, F. Y. Boey, Q. Yan, P. Chen, and H. Zhang (2009) *In situ* synthesis of metal nanoparticles on single-layer graphene oxide and reduced graphene oxide surfaces. *J. Phys. Chem. C.* 113: 10842-10846.
45. Williams, G., B. Seger, and P. V. Kamat (2008) TiO2-graphene nanocomposites. UV-assisted photocatalytic reduction of graphene oxide. *ACS Nano.* 2: 1487-1491.
46. Lightcap, I. V., T. H. Kosel, and P. V. Kamat (2010) Anchoring semiconductor and metal nanoparticles on a two-dimensional catalyst mat. Storing and shuttling electrons with reduced graphene oxide. *Nano Lett.* 10: 577-583.
47. Li, J., D. Kuang, Y. Feng, F. Zhang, Z. Xu, M. Liu, and D. Wang (2013) Green synthesis of silver nanoparticles-graphene oxide nanocomposite and its application in electrochemical sensing of tryptophan. *Biosens. Bioelectron.* 42: 198-206.
48. Gao, N., Y. Chen, and J. Jiang (2013) Ag@Fe2O3-GO nanocomposites prepared by a phase transfer method with long-term antibacterial property. *ACS Appl. Mater. Interfaces.* 5: 11307-11314.
49. Le, A. -T., L. T. Tam, P. D. Tam, P. T. Huy, T. Q. Huy, N. Van Hieu, A. A. Kudrinskiy, and Y. A. Krutyakov (2010) Synthesis of oleic acid-stabilized silver nanoparticles and analysis of their antibacterial activity. *Mater. Sci. Eng. C Mater. Biol. Appl.* 30: 910-916.
50. Guzmán, M. G., J. Dille, and S. Godet (2009) Synthesis of silver nanoparticles by chemical reduction method and their antibacterial activity. *Int. J. Chem. Biomol. Eng.* 2: 104-111.
51. Nishioka, M., M. Miyakawa, H. Kataoka, H. Koda, K. Sato, and T. M. Suzuki (2011) Continuous synthesis of monodispersed silver nanoparticles using a homogeneous heating microwave reactor system. *Nanoscale.* 3: 2621-2626.
52. Chen, P., L. Song, Y. Liu, and Y. -E. Fang (2007) Synthesis of silver nanoparticles by γ-ray irradiation in acetic water solution containing chitosan. *Radiat. Phys. Chem.* 76: 1165-1168.
53. Yang, J., C. Zang, L. Sun, N. Zhao, and X. Cheng (2011) Synthesis of graphene/Ag nanocomposite with good dispersibility and electroconductibility *via* solvothermal method. *Mater. Chem. Phys.* 129: 270-274.
54. Liu, J., W. Dong, P. Zhan, S. Wang, J. Zhang, and Z. Wang (2005) Synthesis of bimetallic nanoshells by an improved electroless plating method. *Langmuir.* 21: 1683-1686.
55. Ahmad, A., P. Mukherjee, S. Senapati, D. Mandal, M. I. Khan, R. Kumar, and M. Sastry (2003) Extracellular biosynthesis of silver nanoparticles using the fungus Fusarium oxysporum. *Colloids Surf. B Biointerfaces.* 28: 313-318.
56. Wang, H., X. Qiao, J. Chen, and S. Ding (2005) Preparation of silver nanoparticles by chemical reduction method. *Colloids Surf. A Physicochem. Eng. Asp.* 256: 111-115.

57. Fayaz, A. M., K. Balaji, M. Girilal, R. Yadav, P. T. Kalaichelvan, and R. Venketesan (2010) Biogenic synthesis of silver nanoparticles and their synergistic effect with antibiotics: A study against gram-positive and gram-negative bacteria. *Nanomed.* 6: 103-109.
58. Krishnaraj, C., E. G. Jagan, S. Rajasekar, P. Selvakumar, P. T. Kalaichelvan, and N. Mohan (2010) Synthesis of silver nanoparticles using Acalypha indica leaf extracts and its antibacterial activity against water borne pathogens. *Colloids Surf. B Biointerfaces.* 76: 50-56.
59. Huang, H. and X. Yang (2004) Synthesis of polysaccharide-stabilized gold and silver nanoparticles: A green method. *Carbohydr. Res.* 339: 2627-2631.
60. Sharma, V. K., R. A. Yngard, and Y. Lin (2009) Silver nanoparticles: Green synthesis and their antimicrobial activities. *Adv. Colloid Interface Sci.* 145: 83-96.
61. Courrol, L. C., F. R. de Oliveira Silva, and L. Gomes (2007) A simple method to synthesize silver nanoparticles by photoreduction. *Colloids Surf. A Physicochem. Eng. Asp.* 305: 54-57.
62. Mafuné, F., J. -Y. Kohno, Y. Takeda, T. Kondow, and H. Sawabe (2000) Formation and size control of silver nanoparticles by laser ablation in aqueous solution. *The J. Physic. Chem B.* 104: 9111-9117.
63. Khaydarov, R. A., R. R. Khaydarov, O. Gapurova, Y. Estrin, and T. Scheper (2008) Electrochemical method for the synthesis of silver nanoparticles. *J. Nanopart. Res.* 11: 1193-1200.
64. Kobayashi, Y., V. Salgueiriño-Maceira, and L. M. Liz-Marzán (2001) Deposition of silver nanoparticles on silica spheres by pretreatment steps in electroless plating. *Chem. Mater.* 13: 1630-1633.
65. Thakkar, K. N., S. S. Mhatre, and R. Y. Parikh (2010) Biological synthesis of metallic nanoparticles. *Nanomed.* 6: 257-262.
66. Martinez-Gutierrez, F., P. L. Olive, A. Banuelos, E. Orrantia, N. Nino, E. M. Sanchez, F. Ruiz, H. Bach, and Y. Av-Gay (2010) Synthesis, characterization, and evaluation of antimicrobial and cytotoxic effect of silver and titanium nanoparticles. *Nanomed.* 6: 681-688.
67. Allsopp, M., A. Walters, and D. Santillo (2007) Nanotechnologies and nanomaterials in electrical and electronic goods: A review of uses and health concerns. *Greenpeace Res. Laboratories, London.*
68. Zhang, D., X. Liu, and X. Wang (2011) Green synthesis of graphene oxide sheets decorated by silver nanoprisms and their anti-bacterial properties. *J. Inorg. Biochem.* 105: 1181-1186.
69. Li, D. G., S. H. Chen, S. Y. Zhao, X. M. Hou, H. Y. Ma, and X. G. Yang (2004) Simple method for preparation of cubic Ag nanoparticles and their self-assembled films. *Thin Solid Films.* 460: 78-82.
70. Li, J. and C. -Y. Liu (2010) Ag/Graphene Heterostructures: Synthesis, characterization and optical properties. *Eur. J. Inorg. Chem.* 2010: 1244-1248.
71. López-Miranda, A., A. López-Valdivieso, and G. Viramontes-Gamboa (2012) Silver nanoparticles synthesis in aqueous solutions using sulfite as reducing agent and sodium dodecyl sulfate as stabilizer. *J. Nanopart. Res.* 14: 1101.
72. Bastús, N. G., F. Merkoçi, J. Piella, and V. Puntes (2014) Synthesis of highly monodisperse citrate-stabilized silver nanoparticles of up to 200 nm: Kinetic control and catalytic properties. *Chem. Mater.* 26: 2836-2846.
73. Shirakawa, H., E. J. Louis, A. G. MacDiarmid, C. K. Chiang, and A. J. Heeger (1977) Synthesis of electrically conducting organic polymers: halogen derivatives of polyacetylene, (CH) x. *J. Chem. Soc. Chem. Commun.* 578-580.
74. Khampieng, T., P. Brikshavana, and P. Supaphol (2014) Silver nanoparticle-embedded poly(vinyl pyrrolidone) hydrogel dressing: Gamma-ray synthesis and biological evaluation. *J. Biomater. Sci. Polym. Ed.* 25: 826-842.
75. Abdelgawad, A. M., S. M. Hudson, and O. J. Rojas (2014) Antimicrobial wound dressing nanofiber mats from multicomponent (chitosan/silver-NPs/polyvinyl alcohol) systems. *Carbohydr. Polym.* 100: 166-178.
76. Chithrani, B. D., A. A. Ghazani, and W. C. Chan (2006) Determining the size and shape dependence of gold nanoparticle uptake into mammalian cells. *Nano Lett.* 6: 662-668.
77. Santra, S., R. Tapec, N. Theodoropoulou, J. Dobson, A. Hebard, and W. Tan (2001) Synthesis and characterization of silica-coated iron oxide nanoparticles in microemulsion: The effect of nonionic surfactants. *Langmuir.* 17: 2900-2906.
78. Xu, G. -N., X. -L. Qiao, X. -L. Qiu, and J. -G. Chen (2008) Preparation and characterization of stable monodisperse silver nanoparticles *via* photoreduction. *J. Chem. Soc. Chem. Commun.* 320: 222-226.
79. Mallik, K., M. Mandal, N. Pradhan, and T. Pal (2001) Seed mediated formation of bimetallic nanoparticles by UV irradiation: A photochemical approach for the preparation of "core-shell" type structures. *Nano Lett.* 1: 319-322.
80. Petit, C., P. Lixon, and M. P. Pileni (1993) *In situ* synthesis of silver nanocluster in AOT reverse micelles. *J. Phys. Chem. B* 97: 12974-12983.
81. Pileni, M. (1997) Nanosized particles made in colloidal assemblies. *Langmuir.* 13: 3266-3276.
82. Chen, Y. -H. and C. -S. Yeh (2002) Laser ablation method: Use of surfactants to form the dispersed Ag nanoparticles. *Colloids Surf. A Physicochem. Eng. Asp.* 197: 133-139.
83. Pyatenko, A., K. Shimokawa, M. Yamaguchi, O. Nishimura, and M. Suzuki (2004) Synthesis of silver nanoparticles by laser ablation in pure water. *Appl. Physics A.* 79.
84. K, H. M., M. G. Naseri, A. R. Sadrolhosseini, A. Dehzangi, A. Kamalianfar, E. B. Saion, R. Zamiri, H. A. Ahangar, and B. Y. Majlis (2014) Silver nanoparticle fabrication by laser ablation in polyvinyl alcohol solutions. *Chinese Phys. Lett.* 31: 077803.
85. Sap-Iam, N., C. Homklinchan, R. Larpudomlert, W. Warisnoicharoen, A. Sereemaspun, and S. Dubas (2010) UV irradiation-induced silver nanoparticles as mosquito larvicides. *J. Appl. Sci. (Faisalabad)* 10: 3132-3136.
86. Henglein, A. and M. Giersig. (1999) Formation of colloidal silver nanoparticles: Capping action of citrate. *J. Phys. Chem. B* 103: 9533-9539.
87. Shin, H. S., H. J. Yang, S. B. Kim, and M. S. Lee (2004) Mechanism of growth of colloidal silver nanoparticles stabilized by polyvinyl pyrrolidone in gamma-irradiated silver nitrate solution. *J. Colloid Interface Sci.* 274: 89-94.
88. Bogle, K. A., S. D. Dhole, and V. N. Bhoraskar (2006) Silver nanoparticles: Synthesis and size control by electron irradiation. *Nanotechnol.* 17: 3204-3208.
89. Prathna, T. C., A. M. Raichur, N. Chandrasekaran, and A. Mukherjee (2013) Sunlight irradiation induced green synthesis of stable silver nanoparticles using citrus limon extract. *Proc. Natl. Acad. Sci. India Sect. B Biol. Sci.* 84: 65-70.
90. Thirumalai Arasu, V., D. Prabhu, and M. Soniya (2010) Stable silver nanoparticle synthesizing methods and its applications. *J. Bio. Sci. Res.* 1: 259-270.
91. Zhang, W., X. Qiao, and J. Chen (2007) Synthesis of silver nanoparticles—Effects of concerned parameters in water/oil microemulsion. *Mater. Sci. Eng. B.* 142: 1-15.
92. Arunachalam, K. D., S. K. Annamalai, A. M. Arunachalam, K. Subashini, and S. Kennedy (2013) Green synthesis of crystalline silver nanoparticles using Indigofera aspalathoides-medicinal plant extract for wound healing applications. *Asian J. Chem.* 25: 311-314.
93. Bhainsa, K. C. and S. F. D'Souza (2006) Extracellular biosynthesis of silver nanoparticles using the fungus Aspergillus fumi-

gatus. *Colloids Surf. B Biointerfaces.* 47: 160-164.
94. Sangeetha, G., S. Rajeshwari, and R. Venckatesh (2011) Green synthesis of zinc oxide nanoparticles by aloe barbadensis miller leaf extract: Structure and optical properties. *Mater Res. Bull*. 46: 2560-2566.
95. Pourjavadi, A. and R. Soleyman (2011) Silver nanoparticles with gelatin nanoshells: Photochemical facile green synthesis and their antimicrobial activity. *J. Nanopart. Res.* 13: 4647-4658.
96. Fan, X., W. Peng, Y. Li, X. Li, S. Wang, G. Zhang, and F. Zhang (2008) Deoxygenation of exfoliated graphite oxide under alkaline conditions: A green route to graphene preparation. *Adv. Mater.* 20: 4490-4493.
97. Stankovich, S., R. D. Piner, S. T. Nguyen, and R. S. Ruoff (2006) Synthesis and exfoliation of isocyanate-treated graphene oxide nanoplatelets. *Carbon* 44: 3342-3347.
98. Gaffet, E., M. Tachikart, O. El Kedim, and R. Rahouadj (1996) Nanostructural materials formation by mechanical alloying: Morphologic analysis based on transmission and scanning electron microscopic observations. *Mater Character.* 36: 185-190.
99. He, F., J. Fan, D. Ma, L. Zhang, C. Leung, and H. L. Chan (2010) The attachment of Fe3O4 nanoparticles to graphene oxide by covalent bonding. *Carbon* 48: 3139-3144.
100. Liu, Q., J. Shi, J. Sun, T. Wang, L. Zeng, and G. Jiang (2011) Graphene and graphene oxide sheets supported on silica as versatile and high-performance adsorbents for solid-phase extraction. *Angew Chem. Int. Ed. Engl.* 50: 5913-5917.
101. Chu, B. H., C. F. Lo, J. Nicolosi, C.Y. Chang, V. Chen, W. Strupinski, S. J. Pearton, and F. Ren (2011) Hydrogen detection using platinum coated graphene grown on SiC. *Sens. Actuators B Chem.* 157: 500-503.
102. Shen, T., J. J. Gu, M. Xu, Y. Q. Wu, M. L. Bolen, M. A. Capano, L. W. Engel, and P. D. Ye (2009) Observation of quantum-Hall effect in gated epitaxial graphene grown on SiC (0001). *Appl. Phys. Lett.* 95: 172105.
103. Samal, M., J. M. Lee, W. I. Park, D. K. Yi, U. Paik, and C. -L. Lee (2011) Surface morphology changes of graphene on flexible PET substrate upon thermal annealing. *J. Nanosci. Nanotechnol*. 11: 10069-10077.
104. Lin, W., R. Zhang, K. -S. Moon, and C. P. Wong (2010) Molecular phonon couplers at carbon nanotube/substrate interface to enhance interfacial thermal transport. *Carbon* 48: 107-113.
105. Tang, X. Z., Z. Cao, H. B. Zhang, J. Liu, and Z. Z. Yu (2011) Growth of silver nanocrystals on graphene by simultaneous reduction of graphene oxide and silver ions with a rapid and efficient one-step approach. *Chem. Commun. (Camb).* 47: 3084-3086.
106. Arco, D., L. Gomez, Y. Zhang, A. Kumar, and C. Zhou (2009) Synthesis, transfer, and devices of single-and few-layer graphene by chemical vapor deposition. *Nanotechnol. IEEE Transactions On.* 8: 135-138.
107. Bao, Q., D. Zhang, and P. Qi (2011) Synthesis and characterization of silver nanoparticle and graphene oxide nanosheet composites as a bactericidal agent for water disinfection. *J. Colloid Interface Sci.* 360: 463-470.
108. Orlita, M., C. Faugeras, J. M. Schneider, G. Martinez, D. K. Maude, and M. Potemski (2009) Graphite from the viewpoint of Landau level spectroscopy: An effective graphene bilayer and monolayer. *Phys. Rev. Lett.* 102: 166401.
109. Bussy, C., H. Ali-Boucetta, and K. Kostarelos (2012) Safety considerations for graphene: Lessons learnt from carbon nanotubes. *Acc. Chem. Res*. 46: 692-701.
110. Marcano, D. C., D. V. Kosynkin, J. M. Berlin, A. Sinitskii, Z. Sun, A. Slesarev, L. B. Alemany, W. Lu, and J. M. Tour (2010) Improved synthesis of graphene oxide. *ACS Nano.* 4: 4806-4814.
111. Hummers Jr, W. S. and R. E. Offeman (1958) Preparation of graphitic oxide. *J. Am. Chem. Soc.* 80: 1339-1339.
112. Silver, S., L. T. Phung, and G. Silver (2006) Silver as biocides in burn and wound dressings and bacterial resistance to silver compounds. *J. Ind. Microbiol. Biotechnol.* 33: 627-634.
113. Kim, J. S., E. Kuk, K. N. Yu, J. -H. Kim, S. J. Park, H. J. Lee, S. H. Kim, Y. K. Park, Y. H. Park, and C. -Y. Hwang (2007) Antimicrobial effects of silver nanoparticles. *Nanomed.* 3: 95-101.
114. Akhavan, O. and E. Ghaderi (2010) Toxicity of graphene and graphene oxide nanowalls against bacteria. *ACS Nano.* 4: 5731-5736.
115. Hu, W., C. Peng, W. Luo, M. Lv, X. Li, D. Li, Q. Huang, and C. Fan (2010) Graphene-based antibacterial paper. *Acs Nano.* 4: 4317-4323.
116. Liu, X. and K. L. Chen (2015) Interactions of graphene oxide with model cell membranes: Probing nanoparticle attachment and lipid bilayer disruption. *Langmuir.* 31: 12076-12086.
117. Chook, S. W., C. H. Chia, S. Zakaria, M. K. Ayob, K. L. Chee, N. M. Huang, H. M. Neoh, H. N. Lim, R. Jamal, and R. M. F. R. A. Rahman (2012) Antibacterial performance of Ag nanoparticles and AgGO nanocomposites prepared *via* rapid microwave-assisted synthesis method. *Nanoscale Res. Lett.* 7: 1-7.
118. Das, M. R., R. K. Sarma, R. Saikia, V. S. Kale, M. V. Shelke, and P. Sengupta (2011) Synthesis of silver nanoparticles in an aqueous suspension of graphene oxide sheets and its antimicrobial activity. *Colloids Surf. B Biointerfaces.* 83: 16-22.
119. Kumar, S. V., N. M. Huang, H. N. Lim, M. Zainy, I. Harrison, and C. H. Chia (2013) Preparation of highly water dispersible functional graphene/silver nanocomposite for the detection of melamine. *Sens. Actuators B Chem.* 181: 885-893.
120. Li, C., X. Wang, F. Chen, C. Zhang, X. Zhi, K. Wang, and D. Cui (2013) The antifungal activity of graphene oxide–silver nanocomposites. *Biomat.* 34: 3882-3890.
121. Zhang, Z., J. Zhang, B. Zhang, and J. Tang (2013) Mussel-inspired functionalization of graphene for synthesizing Ag-polydopamine-graphene nanosheets as antibacterial materials. *Nanoscale.* 5: 118-123.
122. Shen, J., M. Shi, N. Li, B. Yan, H. Ma, Y. Hu, and M. Ye (2010) Facile synthesis and application of Ag-chemically converted graphene nanocomposite. *Nano Res.* 3: 339-349.
123. Xu, W. -P., L. -C. Zhang, J. -P. Li, Y. Lu, H. -H. Li, Y. -N. Ma, W. -D. Wang, and S. -H. Yu (2011) Facile synthesis of silver@ graphene oxide nanocomposites and their enhanced antibacterial properties. *J. Mater. Chem.* 21: 4593-4597.
124. Ma, J., J. Zhang, Z. Xiong, Y. Yong, and X. Zhao (2011) Preparation, characterization and antibacterial properties of silver-modified graphene oxide. *J. Mater. Chem.* 21: 3350-3352.
125. Ocsoy, I., B. Gulbakan, T. Chen, G. Zhu, Z. Chen, M. M. Sari, L. Peng, X. Xiong, X. Fang, and W. Tan (2013) DNA-guided metal-nanoparticle formation on graphene oxide surface. *Adv. Mater.* 25: 2319-2325.
126. Subbiah, R., M. Veerapandian, and K. S Yun (2010) Nanoparticles: Functionalization and multifunctional applications in biomedical sciences. *Curr. Med. Chem.* 17: 4559-4577.
127. Veerapandian, M., M. -H. Lee, K. Krishnamoorthy, and K. Yun (2012) Synthesis, characterization and electrochemical properties of functionalized graphene oxide. *Carbon* 50: 4228-4238.
128. Chen, Y., N. Gao, and J. Jiang (2013) Surface matters: Enhanced bactericidal property of Core–Shell Ag–Fe2O3 nanostructures to their heteromer counterparts from one-pot synthesis. *Small.* 9: 3242-3246.
129. Lan, N. T., D. T. Chi, N. X. Dinh, N. D. Hung, H. Lan, P.A. Tuan, L. H. Thang, N. N. Trung, N. Q. Hoa, T. Q. Huy, N. V. Quy, T. -T. Duong, V. N. Phan, and A. -T. Le (2014) Photochemical decoration of silver nanoparticles on graphene oxide nanosheets and their optical characterization. *J. Alloys Compd.*

615: 843-848.
130. Liu, G., Y. Wang, X. Pu, Y. Jiang, L. Cheng, and Z. Jiao (2015) One-step synthesis of high conductivity silver nanoparticle-reduced graphene oxide composite films by electron beam irradiation. *Appl. Surf. Sci.* 349: 570-575.
131. Sadrolhesseini, A. R., A. Noor, M. Mahdi, A. Kharazmi, A. Zakaria, W. Yunus, and N. Huang (2013) Laser ablation synthesis of silver nanoparticle in graphene oxide and thermal effusivity of nanocomposite. pp. 62-65. *Photonics (ICP), 2013 IEEE 4th International Conference on, IEEE.*
132. Hui, K. S., K. N. Hui, D. A. Dinh, C. H. Tsang, Y. R. Cho, W. Zhou, X. Hong, and H. -H. Chun (2014) Green synthesis of dimension-controlled silver nanoparticle–graphene oxide with in situ ultrasonication. *Acta Materialia.* 64: 326-332.
133. Zainy, M., N. M. Huang, S. Vijay Kumar, H. N. Lim, C. H. Chia, and I. Harrison (2012) Simple and scalable preparation of reduced graphene oxide–silver nanocomposites *via* rapid thermal treatment. *Mater. Lett.* 89: 180-183.
134. Veerapandian, M., H. Y. Kim, Y. -T. Seo, K. -N. Lee, K. Yun, and M. -H. Lee (2014) Metalloid polymer nanoparticle functionalized graphene oxide working electrode for durable glucose sensing. *Mater. Res. Bull.* 49: 593-600.
135. Veerapandian, M. and S. Neethirajan (2015) Graphene oxide chemically decorated with Ag–Ru/chitosan nanoparticles: Fabrication, electrode processing and immunosensing properties. *RSC Adv.* 5: 75015-75024.
136. Wu, Y., W. Xu, Y. Wang, Y. Yuan, and R. Yuan (2013) Silver–graphene oxide nanocomposites as redox probes for electrochemical determination of α-1-fetoprotein. *Electrochim. Acta* 88: 135-140.
137. Wu, M., D. Lu, Y. Zhao, and T. Ju (2013) Facile synthesis of silver-modified functionalised graphene oxide nanocomposite with enhanced antibacterial property. *Micro Nano Lett.* 8: 82-85.